AN ABSTRACT OF THE THESIS OF

DAVID LOUIS SLEGEL (Name) for the DOCTOR OF PHILOSOPHY (Degree)

in Mechanical and Metallurgical Engineering (Major Department) presented on July 12, 1974 (Date)

Title: TRANSIENT HEAT AND MASS TRANSFER IN SOILS IN THE VICINITY OF HEATED POROUS PIPES

Abstract approved: Redacted for Privacy

Lorin R. Davis

Differential equations governing the combined heat and mass transfer in soils are developed. Transient heat, liquid and vapor transfer with phase change is considered. The liquid transfer is treated as a function of the hydraulic conductivity and the gradient of suction potential. The suction potential is considered a function of moisture content and temperature. The hydraulic conductivity is considered a function of moisture content. Vapor transfer is treated as a diffusion process. Vapor density is found as a function of temperature and moisture content by the assumption of local thermodynamic equilibrium.

The governing differential equations are expressed in finite difference form utilizing an implicit central difference scheme for two dimensions. Numerical solutions are obtained through the use of a digital computer.

A steady-state solution is obtained for boundary conditions modeling an experiment. The computer solution is compared to the results of the experiment as a check for the analytical approach.

A soil warming and irrigation system is then modeled for field conditions and results are obtained for various pipe spacings and depths utilizing data for a particular sandy soil and weather data for a particular location. These results are presented as plots of temperature and moisture content. Possible criteria for the optimization of the spacing and depth of the pipes for agricultural purposes are also presented. A possible method for optimizing the effect of the soil warming and irrigation system on the plant environment is therefore described utilizing the computer program to predict temperature and moisture in the vicinity of the heated porous pipes.

Transient Heat and Mass Transfer in Soils in the Vicinity of Heated Porous Pipes

by

David Louis Slegel

A THESIS

submitted to

Oregon State University

in partial fulfillment of
the requirements for the
degree of

Doctor of Philosophy

June 1975

APPROVED:

Redacted for Privacy

Associate Professor of Mechanical and
Metallurgical Engineering

in charge of major

Redacted for Privacy

Head of Department of Mechanical and
Metallurgical Engineering

Redacted for Privacy

Dean of Graduate School

Date thesis is presented July 12, 1974

Typed by Clover Redfern for David Louis Slegel

ACKNOWLEDGEMENT

I would like to express my appreciation to my major professor, Dr. Lorin R. Davis, for his help and encouragement throughout my work at Oregon State University.

I would also like to thank Dr. Larry Boersma and Ali Sepaskhah for their help and cooperation during my work on this thesis.

Financial support for work on this project was provided through a grant by Pacific Power & Light Co., Portland General Electric Co., and the Boeing Co.

TABLE OF CONTENTS

LIST OF TABLES

LIST OF FIGURES

LIST OF SYMBOLS

Latin

c_p	specific heat at constant pressure--cal/g-°K
c_v	specific heat at constant volume--cal/g-°C
D	vapor diffusivity--cm^2/sec
E	evaporation rate--g/cm^3-sec
g	acceleration of gravity--cm/sec^2
G	Gibbs free energy--cal/g
h	enthalpy--cal/g or heat transfer film coefficient--cal/cm^2-sec-°K
h_D	vapor convection coefficient--cm/sec
h_{fg}	heat of vaporization--cal/g
i	vertical unit vector
k	hydraulic conductivity--cm/sec
m_{rain}	precipitation rate--g/cm^2-sec
P	pressure--Dynes/cm^2
q	flux--g/cm^2-sec or cal/cm^2-sec
r	the ratio $\Delta z/\Delta y$
R	Universal gas constant -- cal/g-°K
S	porosity -- cm^3/cm^3
t	time -- sec
T	temperature -- °K

U internal energy--cal/cm^3

y horizontal coordinate

z gravitational potential or the vertical coordinate--cm

Greek

α tortuosity

β dimensionless density

$\bar{\delta}$ dimensionless gradient operator

$\bar{\nabla}$ gradient operator--cm^{-1}

θ water content--cm^3/cm^3

λ thermal conductivity--cal/cm-sec-°K

ρ density--g/cm^3

τ dimensionless time

ϕ total potential--cm

ψ thermodynamic potential of water in soil--cm

Δt time increment--sec

Δz vertical distance between nodes

Subscripts

a air

ℓ liquid

m vertical node index

n horizontal node index

s surface

sat	saturated vapor
v	vapor
vo	vapor in air-filled pore
w	pure liquid water
∞	atmospheric condition

Superscripts

'	denotes a dimensionless variable
*	denotes that the variable is at the incremented time
$\rightarrow$	denotes a vector

TRANSIENT HEAT AND MASS TRANSFER IN SOILS IN THE VICINITY OF HEATED, POROUS PIPES

I. INTRODUCTION

General Background

Due to the increasing demand for electrical energy, it has been estimated that the generating capacity of the United States will have to double every ten years. Since most of this increase in generating capacity will be from thermal plants, and since the efficiency of such plants is limited (33 to 40%), the amount of heat rejected to the environment will increase greatly. The environmental impact of this rejected heat has been of increasing concern. Introduction of warm condenser cooling water to rivers has already been limited. Use of the ocean as a sink for the rejected heat has been considered, but licensing procedures require extensive study of the effect and dispersal of this heat. Another method of rejecting the "waste heat" is through the use of a cooling tower. While all of these methods provide an efficient means of dispersing the waste heat, none offers any beneficial use of the waste heat itself.

Many beneficial uses of the waste heat have been suggested. Among these are warming of lakes for recreational purposes, warming of ponds for commercial rearing of fish or algae, industrial, commercial and residential heating, and heating for agricultural

purposes, etc. Among the agricultural uses are irrigation and heating of the crop environment. This heating and irrigation can be accomplished in greenhouses or in open fields. Heating of the surrounding air has been reported to increase crop yields by fifty percent, while heating the soil may result in another fifty percent increase (1). These increases are due to the enhanced growing conditions and to the prolonged growing period possible with warmer crop surroundings.

Heating and irrigation of the soil were proposed to be accomplished by means of a system of parallel porous pipes buried at uniform spacing and depth (1). Subsurface heating and irrigation is more expensive than surface heating and irrigation because of the cost of installing the subsurface piping system. However, subsurface irrigation and heating is more beneficial for several reasons. First is the fact that surface heating would result in little warming of the soil, while most of the heat would be lost to the atmosphere. Surface irrigation with warm water would result in high evaporation rates and, consequentially, large water losses. Subsurface heating and irrigation result in much smaller water loss and much greater heating of the soil.

Since the use of a soil warming and irrigation system would be on an economic basis, it would be desired to optimize the benefit of the system. Since a major part of the cost of a soil warming and

irrigation system is the cost of installation, it is desirable to find an optimum pipe spacing and depth before the system is installed.

Heat Transfer in Soils--Background

In order to optimize the pipe spacing and depth, one must find the effects of the subsurface system of pipes. One method of evaluating the effects of a soil warming and irrigation system is to find the temperature and moisture content distributions in the vicinity of the pipes by analytical means. A classic example of past attempts to find the temperature distribution due to buried cables is found in many heat transfer texts. In the solution of this example it is assumed that the thermal conductivity is constant, that the soil surface is at constant temperature, that the soil is a semi-infinite solid, and that convection in the soil is negligible (2, for an example). The temperature due to a source in an infinite solid at position $y = -h$ is

$$T = C - \frac{q}{2\pi\lambda} \ln((x^2+(h+y)^2)^{1/2}) ,$$

while the temperature due to a heat sink at position $y = +h$ is

$$T = C + \frac{q}{2\pi\lambda} \ln((x^2+(h-y)^2)^{1/2}) .$$

The temperature due to the presence of a source and sink located at $-h$ and $+h$ respectively is the sum of these two temperatures and is

$$T = T_s + \frac{q}{4\pi\lambda} \ln\left[\frac{x^2+(h-y)^2}{x^2+(h+y)^2}\right],$$

where T_s is the temperature at position $y = 0$. This superposition is referred to as the method of images. The temperature at $x = 0$ and $y = -h+R$ is the temperature of the surface of a pipe of radius R. It is denoted by T_o and is $T_o - T_s = \frac{q}{2\pi\lambda} \ln(2h/R-1)$. The heat flux, q, may be eliminated and the temperature written as

$$\frac{T-T_s}{T_o-T_s} = \frac{\ln\left[\frac{x^2+(h-y)^2}{x^2+(h+y)^2}\right]}{2\ln(2h/R-1)}.$$

This equation describes the temperature distribution of a semi-infinite solid whose surface is maintained at T_s and contains a pipe at a position of $x = 0$ and $y = -h$, where the pipe surface temperature is maintained at T_o. The solution is valid for steady-state and for constant thermal conductivity only.

Kendricks and Havens (3) have utilized this approach and superposition to obtain temperature distributions for a large number of cables buried at a uniform spacing and depth. Kendricks and Havens expressed the temperature as

$$\frac{T-T_s}{T_o-T_s} = \frac{0.5 \sum_{n=-N}^{N} \ln\left[\frac{(nS+x)^2+(h-y)^2}{(nS+x)^2+(h+y)^2}\right]}{\ln(2h/R-1) + \sum_{n=1}^{N} \ln\left[\frac{(nS)^2+(2h-R)^2}{(nS)^2+R^2}\right]},$$

where S is the pipe spacing and h is the pipe depth. While this equation may given an indication of the heating effect of a system of buried cables, it is felt that it has serious shortcomings. Among these shortcomings are the assumption of constant thermal conductivity, neglecting convection in the soil, the assumption of steady-state, and the lack of a method for specifying the surface temperature.

In order to adequately assess the effects of a soil warming and irrigation system, it was felt that combined heat and mass transfer in soils must be analyzed, and that heat and mass transfer at the soil surface must be considered. In order to analyze the irrigation effects and to specify the convective heat transfer and evaporation in the soil, equations governing the mass fluxes had to be developed.

The Mass Flux Equations--Background

In order to determine mass flux, a model governing flow in the particular media was developed. For many fluids the Newtonian model suffices. The Newtonian model assumes the shear stress to be proportional to the fluid shear rates. Other models, such as the Powell-Eyring or the power law, express fluid stress as non-linear functions of shear rate. The model for the shear stress is substituted into the momentum equation and a partial differential equation with velocity as the dependent variable is obtained. The fluid flux may then be found for a given set of boundary conditions.

In contrast to fluid flow, mass flux in porous media is expressed in terms of the gradients of temperature and moisture content, or is expressed in terms of the gradient of the total potential of the liquid in the porous media. This treatment is necessary because the structure of porous media is normally too complex to describe mathematically. To apply such complex boundary conditions to the momentum equation would be extremely difficult, if not impossible. Instead, a semi-empirical approach is used, where the constant of proportionality is found experimentally. When the gradient of potential is used, the constant is referred to as the hydraulic conductivity.

In the field of liquid transfer in porous media, much work has been done for isothermal, saturated soils. For these conditions the governing equation is simply the Laplace equation with the potential the dependent variable. For unsaturated media, the hydraulic conductivity is a function of moisture content. The continuity equation therefore becomes an implicit equation with moisture content as the dependent variable. Non-isothermal conditions are more difficult because the continuity equation for liquid transfer is then coupled to the energy equation.

Since the transfer of vapor through the soil is a diffusion process in the soil pores, vapor flux has been modeled by the diffusion equation modified to include the presence of the porous media and the liquid moisture. Since the vapor density is dependent on temperature

and moisture content, the vapor, liquid and heat transfer equations are all coupled.

One approach to mass transfer in porous media, based on classical liquid and vapor flux relationships, has been developed by Philip and de Vries (4). This approach utilizes Darcy's law for liquid flux, which is

$$\bar{q}_\ell = -\rho_w k \bar{\nabla}\phi .$$

A diffusion equation was used for vapor flux and is

$$\bar{q}_v = -D\bar{\nabla}\rho_{vo} .$$

In order to express the flux in terms of gradients of moisture content and temperature, Philip and de Vries transformed the equations to the form,

$$\bar{q}_\ell = -D_{T\ell}\bar{\nabla}T - D_{\theta\ell}\bar{\nabla}\theta - \rho_w k\, i ,$$

where

$$D_{T\ell} = \rho_w k\left(\frac{\partial\psi}{\partial T}\right)_\theta ,$$

and

$$D_{\theta\ell} = \rho_w k\left(\frac{\partial\psi}{\partial\theta}\right)_T .$$

These equations for the liquid and vapor fluxes were then combined and substituted into the continuity equation for total moisture transport. Subsequently, de Vries (5) utilized the equations for liquid and

vapor fluxes and separate continuity equations for the liquid and vapor phases to develop equations for evaporation rate and liquid moisture content. He then developed an energy equation utilizing the flux equations. Local thermodynamic equilibrium was then assumed to obtain an expression for vapor density in terms of the potential and temperature. The equations so developed formed a set of equations from which temperature and moisture content could be obtained. The equations were then simplified by de Vries to correspond to a steady-state, one-dimensional case in which the gradients of temperature and moisture content were expressed as functions of the diffusion coefficients and the heat and mass fluxes.

Fritton et al. (6), using measured diffusion coefficients, compared the results of the simplified equations of Philip and de Vries to experimental results for soil exposed to several surface conditions. To obtain agreement between experimental and theoretical results the authors divided the measured water diffusivity by factors of 35 and 10. The authors attributed this discrepancy to hysteresis in the water tension curve and to the temperature dependence of the hydraulic conductivity.

A second approach to heat and mass transfer in soils has been developed from the theory of the thermodynamics of irreversible processes. Cary and Taylor (7, 8) developed equations using this approach for the flux of heat and moisture in saturated and

unsaturated soils, and have experimentally found the phenomenological coefficients for various soils. Cary (9) extended these experiments and equations to liquid, vapor and heat transfer in soils. The flux equations were not, however, applied to continuity or energy equations.

The equations of Philip and de Vries and those of Cary and Taylor are expressed as functions of the gradient of moisture content and temperature, are very complex and are not readily solved. Furthermore, it is felt that the discrepancies between theory and experiment mentioned by Fritton may have been caused by inappropriate attempts to simplify the one-dimensional equations of Philip and de Vries. (Fritton assumed constant temperature in his calculations.)

Present Investigation

The main objective of this investigation was to develop a numerical method for the solution of the transient equations governing combined heat and mass transfer in soils. The mass fluxes were expressed in terms of the gradient of potential for liquid flux and in terms of the gradient of density for vapor flux. The data for suction potential and for hydraulic conductivity used in this investigation were measured values for a particular sandy soil and varied with moisture content. An experiment was modeled by the computer program to verify its validity.

The purpose of the development of the computer program was to model a subsurface heating and irrigation system in order to be able to optimize the spacing and depth of the pipes comprising the system. Temperature and moisture content distributions are presented for several pipe spacings and depths. Some possible optimization criteria are also calculated and presented.

Although the equations governing heat and mass transfer in soils were developed for the general case, the scope of this investigation was limited to the case of two-dimensional heat and mass transfer by neglecting axial gradients. Axial temperature gradients could be made small by large flow rates in the heating pipe. Axial moisture content gradients are expected to be small because the system would be designed to provide uniform irrigation rates along the length of the pipe. A system that did not irrigate uniformly along the pipe would cause high and low moisture content in the soil and would therefore be undesirable. Although there would be many difficulties in developing a piping mechanism that could carry large flow rates while allowing a reasonably constant water loss along its length, such a system was assumed feasible. It was then thought that neglecting the axial heat and mass transfer would induce little error because the axial temperature and moisture content gradients were expected to be small.

Another simplification has been to neglect the absorption of moisture by plant roots. The inclusion of this factor would present no

great difficulty in the development of the computer program. However, the development of a model for rate of absorbtion of moisture as a function of position in the soil or the measurement of the absorbtion rates was beyond the scope of this investigation. The effect of foliage above the surface was also neglected. The effect of both these simplifications is to increase the moisture loss at the surface instead of distributing the loss over the root zone.

II. EQUATIONS AND SOLUTION METHOD

Development of Equations

Liquid flux in porous media can be expressed using Darcy's law (10) as

$$\bar{q}_\ell = -\rho_w k \bar{\nabla} \phi \,, \tag{1}$$

where ρ_w is the density of water, $\bar{q}_\ell$ is the liquid flux, k is the hydraulic conductivity of the soil, and ϕ is the total potential of the liquid in the soil. The total potential, ϕ, is the sum of the gravitational and suction potentials, z and ψ respectively. The suction potential is a function of the surface tension of water, the moisture content of the soil, and the size and shape distribution of the soil particles. The hydraulic conductivity of the soil is similarly dependent on the viscosity of water, the moisture content of the soil and the size and shape distribution of the soil particles. The potential is therefore a measured property of a particular soil and is dependent on moisture content and temperature. The hydraulic conductivity is also a measured property and is dependent on moisture content and temperature. The temperature dependence of hydraulic conductivity has been neglected as being less important the the dependence of moisture content. Although inclusion of the temperature

dependence of hydraulic conductivity was desired, the empirical formula used for hydraulic conductivity did not provide for temperature dependence.

Vapor flux has been treated as a diffusion process. The diffusion relationship is

$$\bar{q}_v = -D\bar{\nabla}\rho_{vo} , \qquad (2)$$

where ρ_{vo} is the vapor density in the soil pore, and D is the vapor diffusivity. Hanks (11) expressed vapor flux for constant temperature as

$$q_x = -a(S-\theta)\frac{D_a M}{RT}\frac{P}{P-P_v}\frac{\partial P_v}{\partial x}$$

which for an ideal gas is equivalent to

$$q_x = -a(S-\theta)D_a\frac{P}{P-P_v}\frac{\partial \rho_{vo}}{\partial x} \qquad (3)$$

where S is the soil porosity, cm^3/cm^3, θ is the soil moisture content, cm^3/cm^3, D_a is the diffusivity of vapor in air, and a is the tortuosity. Due to the low vapor pressures considered (P_{sat} was less than 0.065 atm.), the term, $P/(P-P_v)$, was neglected. Hanks set a equal to 0.66 and calculated the ratio of measured to calculated flow rates for dry soils. His ratios were consistently

higher than unity. Hanks' calculations for the results of other authors yielded ratios for moist soils as high as 11.0. Due to the lack of data for the particular soil modeled and to the uncertainty in the results of the formula, the tortuosity, α, was assumed in this investigation to be unity. According to Hanks the vapor diffusivity in air is

$$D_a = 0.239 \frac{P_o}{P} \left(\frac{T}{281}\right)^{2.3} ,$$

where P_o is the standard atmospheris pressure. For $P = P_o$, comparison of Equations 2 and 3 yields

$$D = 0.239(S-\theta)(T/281)^{2.3} \tag{4}$$

The continuity equations for the vapor and liquid phases are

$$E = \frac{\partial \rho_v}{\partial t} + \bar{\nabla} \cdot \bar{q}_v , \tag{5}$$

and

$$-E = \frac{\partial \rho_\ell}{\partial t} + \bar{\nabla} \cdot \bar{q}_\ell , \tag{6}$$

where E is the evaporation rate, g/cm^3-sec. The vapor density is equal to the product of the density in a pore and the pore fraction. Therefore,

$$\rho_v = (S-\theta)\rho_{vo} .$$

Similarly the liquid density is

$$\rho_\ell = \rho_w \theta$$

Substitution of the above two equations into Equations 5 and 6 yields after expansion

$$E = -\rho_{vo} \frac{\partial \theta}{\partial t} + (S-\theta) \frac{\partial \rho_{vo}}{\partial t} + \bar{\nabla} \cdot \bar{q}_v , \tag{7}$$

and

$$-E = \rho_w \frac{\partial \theta}{\partial t} + \bar{\nabla} \cdot \bar{q}_\ell \tag{8}$$

Since $\rho_{vo} \ll \rho_w$, the first term on the right side of Equation 7 was neglected. After substitution for the fluxes, Equations 7 and 8 are rewritten as

$$E = (S-\theta) \frac{\partial \rho_{vo}}{\partial t} - \bar{\nabla} \cdot D \bar{\nabla} \rho_{vo} \tag{9}$$

$$-E = \rho_w \frac{\partial \theta}{\partial t} - \rho_w \bar{\nabla} \cdot k \bar{\nabla} \phi \tag{10}$$

The energy equation was written as

$$\bar{\nabla} \cdot \lambda \bar{\nabla} T = \frac{\partial}{\partial t} (\rho_\ell U_\ell + \rho_v U_v + \rho_{soil} U_{soil} + \phi) + \bar{\nabla} \cdot (\bar{q}_\ell h_\ell + \bar{q}_v h_v) \tag{11}$$

where T is the temperature, λ is the thermal conductivity, U is the internal energy, and h is the enthalpy. Since the potential,

ϕ, is small for the range of moisture content considered, it was neglected. Expanding Equation 11, substituting Equations 9 and 10 and the relations, $h_{fg} = h_v - h_\ell$, and $U = h - P/\rho$, results in

$$\bar{\nabla} \cdot \lambda \bar{\nabla} T = \rho_\ell \frac{\partial U_\ell}{\partial t} + \rho_v \frac{\partial U_v}{\partial t} + \rho_{soil} \frac{\partial U_{soil}}{\partial t} + h_{fg} E + \bar{q}_\ell \cdot \bar{\nabla} h_\ell$$

$$+ \bar{q}_v \cdot \bar{\nabla} h_v - P_v/\rho_v \frac{\partial \rho_v}{\partial t} - P_\ell/\rho_\ell \frac{\partial \rho_\ell}{\partial t} \qquad (12)$$

The last two terms on the right side of Equation 12 represent mechanical work and were neglected because of their small magnitude. Substitution for h and U in terms of the specific heats and substitution for the liquid density yields

$$\bar{\nabla} \cdot \lambda \bar{\nabla} T = (\rho_w c_{v_\ell} \theta + \rho_{soil} c_{v_{soil}} + \rho_v c_{v_v}) \frac{\partial T}{\partial t}$$

$$+ \bar{q}_\ell \cdot c_{v_\ell} \bar{\nabla} T + \bar{q}_v \cdot c_{p_v} \bar{\nabla} T + h_{fg} E \qquad (13)$$

After substitution for the fluxes, the terms, $\rho_v c_{v_v}$ and $c_{p_v} D \bar{\nabla} \rho_{vo} \cdot \bar{\nabla} T$ are neglected because $\rho_v c_{v_v} \ll \rho_w c_{v_\ell}$. Equation 13 then becomes

$$\bar{\nabla} \cdot \lambda \bar{\nabla} T = (\rho_w c_{v_\ell} \theta + \rho_{soil} c_{v_{soil}}) \frac{\partial T}{\partial t}$$

$$+ h_{fg} E - \rho_w c_{p_\ell} k \bar{\nabla} \phi \cdot \bar{\nabla} T \qquad (14)$$

In order to determine vapor density as a function of moisture content and temperature, local thermodynamic equilibrium is assumed. The Gibbs' free energy of the vapor is

$$G_v = G_o + RT \ln(P_v/P_{sat}) ,$$

where G_o is the Gibbs' free energy of pure water at the temperature of the soil and P_{sat} is the saturated vapor pressure at the same temperature. The Gibbs' free energy of the liquid in the soil is

$$G_\ell = G_o + \psi g .$$

Since the two phases are in equilibrium, $G_v = G_\ell$, and

$$RT \ln(P_v/P_{sat}) = \psi g,$$

or

$$\frac{P_v}{P_{sat}} = e^{\psi g/RT} .$$

Assuming the vapor to be an ideal gas, $P = \rho RT$. Since the temperature at a point is the same for the liquid and vapor phases, P/ρ = constant, and

$$\rho_{vo} = \rho_{sat} e^{\psi g/RT} \qquad (15)$$

Non-Dimensional Equations

In order to non-dimensionalize Equations 9, 10, 14, and 15, the following dimensionless variables were defined.

$$
\begin{aligned}
D' &= D\Delta t/\Delta z^2 \\
E' &= E\Delta t/\rho_w \\
h'_{fg} &= h_{fg}/c_\ell \Delta T \\
k' &= k\Delta t/\Delta z \\
R' &= R\Delta T/g\Delta z \\
T' &= T/\Delta T \\
\beta &= \rho_{vo}/\rho_w \\
\beta c_{soil} &= \rho_{soil} c_{soil}/\rho_w c_{v_\ell} \\
\beta_{sat} &= \rho_{v_{sat}}/\rho_w \\
\bar{\delta} &= \bar{\nabla}\Delta z \\
\lambda' &= \lambda\Delta t/\rho_w c_{v_\ell} \Delta z^2 \\
\psi' &= \psi/\Delta z \,,
\end{aligned}
\tag{16}
$$

where Δz, Δt and ΔT are arbitrary increments of length, time and temperature, respectively.

Substitution into Equations 9 and 10 and multiplication by $\Delta t/\rho_w$ yields

$$
E' = (S-\theta)\frac{\partial \beta}{\partial t} - \bar{\delta} \bullet D' \bar{\delta} \beta \,, \tag{17}
$$

and

$$-E' = \frac{\partial \theta}{\partial t} - \bar{\delta} \bullet k'(\bar{\delta}\psi + i) \quad . \tag{18}$$

Substituting into Equation 15 and multipliying by $\Delta t / \rho_w c_{v_\ell} \Delta T$ yields

$$\bar{\delta} \bullet \lambda' \bar{\delta} T' = (\theta + \beta c_{soil}) \frac{\partial T'}{\partial \tau} + h'_{fg} E' - k'(\bar{\delta}\psi' + i) \bullet \bar{\delta} T' \tag{19}$$

Equation 16 becomes

$$\beta = \beta_{sat} \, e^{\psi'/R'T'} \tag{20}$$

Finite Difference Equations

Due to the non-linear nature of Equations 17, 18, 19 and 20, and the fact that they are coupled, no attempt was made to obtain a closed form solution. Instead, a numerical method was employed. This method consisted of approximating the temperature and moisture content distributions by discrete values at a set of grid points. The differential equations were then approximated by finite difference equations utilizing the discrete values.

A rectangular coordinate system was chosen with z the vertical and y the horizontal coordinates. In order to express the equations in finite difference form, the coordinates, z and y, were expressed as

$$z = (m-1)\Delta z$$

$$y = (n-1)\Delta y .$$

In order to develop the finite difference equations, the spacial derivatives were written using a central difference scheme whereby

$$\frac{\partial T}{\partial z} \sim [T_{m+\frac{1}{2}, n} - T_{m-\frac{1}{2}, n}]/\Delta z,$$

or

$$\frac{\partial \theta}{\partial y} \sim [\theta_{m, n+\frac{1}{2}} - \theta_{m, n-\frac{1}{2}}]/\Delta y.$$

For the time derivatives a backward difference scheme was used whereby

$$\left.\frac{\partial T}{\partial t}\right|_{\tau+1, y, z} = T^*_{m, n} - T_{m, n}$$

where T^* denotes the temperature at the time, $\tau+1$, and where all spacial derivatives were written at the incremented time, $\tau+1$. Using the above approach, Equation 17 is expressed in finite difference form as

$$E^*_{m, n} = (S-\theta^*_{m, n})(\beta^*_{m, n} - \beta_{m, n}) - D^*_{m+\frac{1}{2}, n}(\beta^*_{m+1, n} - \beta^*_{m, n})$$
$$+ D^*_{m-\frac{1}{2}, n}(\beta^*_{m, n} - \beta^*_{m-1, n}) - r^2 D^*_{m, n+\frac{1}{2}}(\beta^*_{m, n+1} - \beta^*_{m, n})$$
$$+ r^2 D^*_{m, n-\frac{1}{2}}(\beta^*_{m, n} - \beta^*_{m, n-1}) \qquad (21a)$$

where all quantities are dimensionless, $r = \Delta z/\Delta y$ and the prime superscript has been deleted. After solving for $\theta^*_{m,n}$, the finite difference form of Equation 18 is

$$\theta^*_{m,n} = \theta_{m,n} - E^*_{m,n} + k^*_{m+\frac{1}{2},n}(\psi^*_{m+1,n} - \psi^*_{m,n+1}) - k^*_{m-\frac{1}{2},n}(\psi^*_{m,n} - \psi^*_{m-1,n+1}) + r^2 k^*_{m,n+\frac{1}{2}}(\psi^*_{m,n+1} - \psi^*_{m,n}) - r^2 k^*_{m,n-\frac{1}{2}}(\psi^*_{m,n} - \psi^*_{m,n-1}) \quad (22a)$$

Due to the dependence of hydraulic conductivity, k, and suction potential, ψ, on the moisture content, θ, Equation 22 was found to be unstable. It was necessary, therefore, to utilize an iterative scheme to obtain a value of $\theta^*_{m,n}$ which would satisfy Equation 22. The scheme used is as follows: given an estimate of moisture content, θ, calculate a predicted value, θ_p, with Equation 22; the next estimate, θ_e, is then

$$\theta_e = (1.-F)\theta + F\theta_p ;$$

iterate until θ_e reaches a constant value. The values of F used were found to depend on moisture content and were valid for the given choice of Δz and Δt only. Expressing Equation 19 in finite difference form and solving for $T^*_{m,n}$ yields

$$T^*_{m,n} = [T_{m,n}(\theta^*_{m,n} + \beta c_{soil}) + h_{fg}E^*_{m,n}$$

$$+ k^*_{m,n}(\psi^*_{m+1,n} - \psi^*_{m-1,n} + 2)(T^*_{m+1,n} - T^*_{m-1,n})/4$$

$$+ r^2 k^*_{m,n}(\psi^*_{m,n+1} - \psi^*_{m,n-1})(T^*_{m,n+1} - T^*_{m,n-1})/4$$

$$+ \lambda^*_{m+\frac{1}{2},n} T^*_{m+1,n} + \lambda^*_{m-\frac{1}{2},n} T^*_{m-1,n}$$

$$+ r^2 \lambda^*_{m,n+\frac{1}{2}} T^*_{m,n+1} + r^2 \lambda^*_{m,n-\frac{1}{2}} T^*_{m,n-1}] \tag{23a}$$

$$/ [\theta^*_{m,n} + \beta c_{soil} + \lambda^*_{m+\frac{1}{2},n} + \lambda^*_{m-\frac{1}{2},n} + r^2 \lambda^*_{m,n+\frac{1}{2}} + r^2 \lambda^*_{m,n-\frac{1}{2}}]$$

Boundary Conditions

In order to solve the partial differential equations describing heat and mass transfer in soils, appropriate boundary conditions must be specified. For the present investigation several types of boundary conditions were used. The vertical boundaries were treated by specifying insulated boundaries making use of symmetry. Symmetry arises from the assumption that a great many pipes are buried at uniform spacing and depth. Since the conditions on either side of the pipe are identical, there exists a vertical line of symmetry passing through the centerline of the pipe. Another line of symmetry is parallel to the first and lies midway between the pipes. Since no flux passes through these lines of symmetry, they are equivalent to

insulated boundaries. Inclusion of the insulated boundaries or lines of symmetry in the finite difference equations was accomplished by creating a set of false nodes lying outside the boundary. Assuming the boundary to be at the grid index m, the temperature and moisture contents at the false nodes at positions, m+1, are set equal to the temperatures and moisture contents at position, m-1. The gradients perpendicular to the boundary are then zero because central difference approximations were used for the spacial derivatives and because the gradient at the boundary is therefore approximated by the difference in two identical values. Since the insulated boundaries or symmetrical boundaries are represented by the gradients being zero perpendicular to the boundary, the false node completely satisfies the boundary condition and no additional derivation is needed.

Two horizontal boundary conditions must be specified. One must either specify the fluxes at the boundary or specify the temperature and moisture content at the boundary. An insulated lower boundary was presumed for the test case and constant temperature and moisture content were specified for the simulation of the soil warming and irrigation system. The assumed constant temperature boundary condition was 10 C at a depth of 1350 cm. Although this assumption seems somewhat arbitrary, the temperature corresponds to measured temperatures (12). Furthermore, it was thought that the

assumption of constant temperature would be of minimal effect because of the great depth at which it was assumed.

The third boundary condition for the moisture content was one of saturation at a depth of 200 cm. It was chosen to represent a typical water table level. No effort was made to verify the constant moisture content boundary condition through use of the computer program because it was felt that factors such as nearby lakes or rivers and underlying rock strata would be of major importance in determining the water table level. It was therefore felt that for accurate modeling of soil warming and irrigation systems, the water table level should be measured for the location of interest.

The fourth boundary condition specified was at the surface of the soil. Since the temperature and moisture content could not be assumed constant at the surface, the fluxes were specified in terms of the surface temperature, the surface moisture content, the atmospheric conditions, and the surface film coefficients. The fluxes so specified were

$$q_v = h_D(\beta_s T_s / T_\infty - \beta_\infty)$$

$$q_\ell = -m_{rain}$$

$$q_{heat} = \epsilon\sigma T_s^4 + h(T_s - T_\infty) - \epsilon q_{solar} - \epsilon q_{atm} ,$$

where the subscript, ∞, denotes atmospheric conditions and the

subscript, s, denotes the surface condition, and q_{atm} denotes the atmospheric radiation. The radiative heat fluxes were determined from empirical formulas which were functions of the amount of cloud cover, atmospheric temperature and relative humidity. The vapor convective film coefficient was determined by modifying an empirical formula for evaporation rate from a lake. The heat transfer film coefficient was found by the analogy between heat and vapor transfer. The empirical formulas for the radiative fluxes and the film coefficients are presented in Appendix I.

Equations 21, 22, and 23 were modified to include the boundary conditions at the soil surface. Using a node height of $\Delta z/2$ and placing the node point on the surface resulted in the following modified equations for the surface.

$$E^*_{m,n} = (S-\theta^*_{m,n})(\beta^*_{m,n}-\beta_{m,n}) + 2h_D(\beta^*_{m,n}-\beta^*_{\infty}) + 2D^*_{m-\frac{1}{2},n}(\beta^*_{m,n}-\beta^*_{m-1,n}) - r^2D^*_{m,n+\frac{1}{2}}(\beta^*_{m,n+1}-\beta^*_{m,n}) + r^2D^*_{m,n-\frac{1}{2}}(\beta^*_{m,n}-\beta^*_{m,n-1}) \quad (21b)$$

$$\theta^*_{m,n} = \theta_{m,n} - E^*_{m,n} + 2m^*_{rain} - 2k^*_{m-\frac{1}{2},n}(\psi^*_{m,n}-\psi^*_{m-1,n}+1) + r^2k^*_{m,n+\frac{1}{2}}(\psi^*_{m,n+1}-\psi^*_{m,n}) - r^2k_{m,n-\frac{1}{2}}(\psi^*_{m,n}-\psi^*_{m,n-1}) \quad (22b)$$

$$T^*_{m,n} = [T_{mn}(\theta^*_{m,n}+\beta c_{soil}) + h_{fg}E^*_{m,n} - \epsilon\sigma T^4_{m,n} + 2hT^*_\infty$$

$$+ 2q^*_{solar} + 2q^*_{atm} + 2m^*_{rain}T^*_\infty + 2\lambda^*_{m-\frac{1}{2},n}T^*_{m-1,n}$$

$$+ r^2\lambda^*_{m,n+\frac{1}{2}}T^*_{m,n+1} + r^2\lambda^*_{m,n-\frac{1}{2}}T^*_{m,n-1}$$

$$+ r^2k^*_{m,n}(\psi^*_{m,n+1}-\psi^*_{m,n-1})(T^*_{m,n+1}-T^*_{m,n-1})/4$$

$$+ 2k^*_{m-\frac{1}{2},n}(\psi^*_{m,n}-\psi^*_{m-1,n}+1)(T^*_{m,n}-T^*_{m-1,n})]$$

$$[\theta^*_{m,n}+\beta c_{soil} + \epsilon\sigma T^{*3}_{m,n} + 2h + 2m_{rain} + 2\lambda^*_{m-\frac{1}{2},n}$$

$$+ r^2\lambda_{m,n+\frac{1}{2}} + r^2\lambda^*_{m,n-\frac{1}{2}}] \qquad (23b)$$

Order of Calculation

The previous difference equations, having been written using a backward difference scheme for time derivatives, are implicit in form and must be solved by iterative methods. In this investigation, the steady-state term of the evaporation rate was first calculated from Equations 20 and 21. The temperatures and transient term of the evaporation rate were then calculated. The moisture contents were then obtained from Equations 22. The entire process was then repeated until the temperature and moisture content arrays converged within a specified amount of error. Calculation was then initiated for the next time step. The computer program so developed is listed in Appendix III with sample input data.

III. RESULTS

Test Case

The computer program was run for the case of an insulated box of soil open to the atmosphere at the top to verify the computational method and check the validity of the equations used. The box was assumed to be filled with a sandy soil and exposed to the atmosphere at the surface. A warm, porous pipe was placed on one wall at a depth of 32 cm. The particular configuration chosen represented an experiment conducted by Sepaskhah (13). Selected results of the experiment appear in Figures 1 and 2 as underlined values. In order to agree with the experiment, the pipe temperature was chosen to be 29 C, the moisture content of the soil adjacent to the pipe was 0.27 cm^3/cm^3, and the atmospheric conditions were 22.7 C and 70% relative humidity. For the test case radiation at the surface was neglected due to the small temperature difference between the soil surface and the surroundings. The node size for the test case was 4.0 cm by 4.0 cm. The computer program was run until the temperatures and moisture contents converged to the steady-state values. The results of this case are presented as isotherms and lines of constant moisture content on Figures 1 and 2, respectively. An additional check was obtained by calculating the temperatures for the same configuration for constant moisture content of 0.27 cm^3/cm^3. The

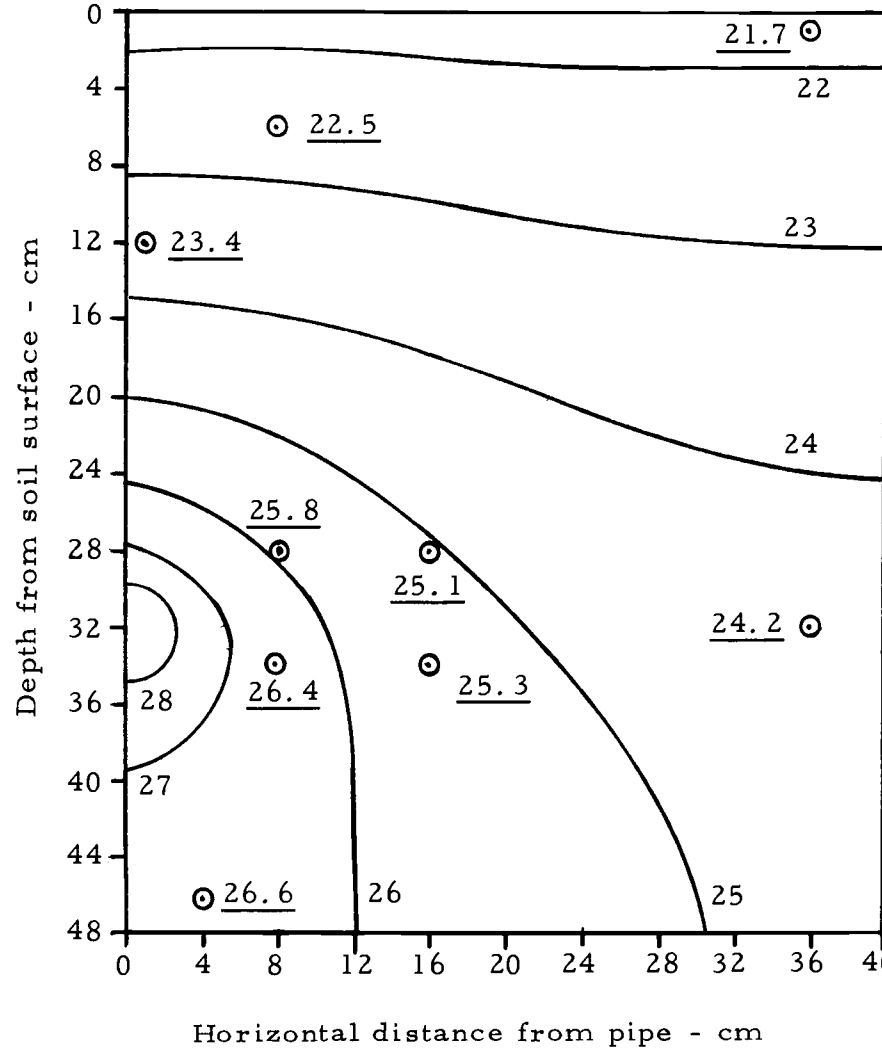

Figure 1. Comparison of calculated temperature (°C) with experimental values From Reference 13.

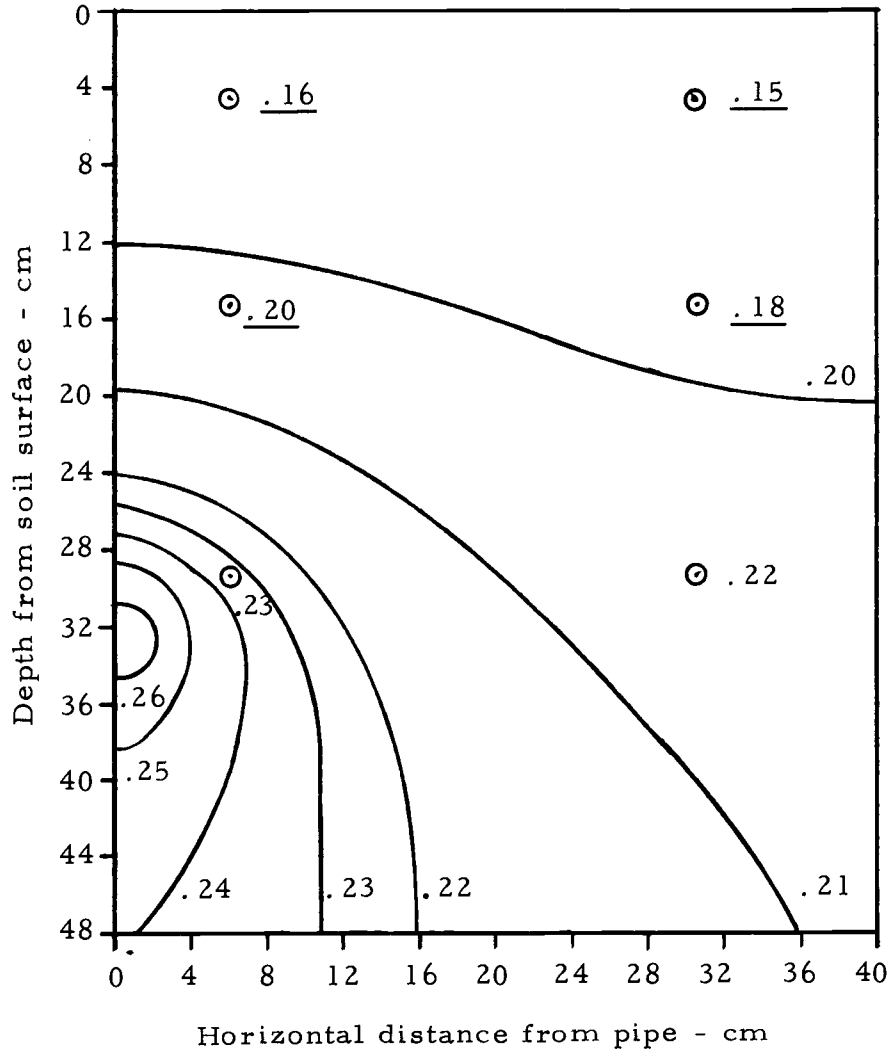

Figure 2. Comparison of calculated moisture content (cm^3/cm^3) with experimental values From Reference 13.

results of these calculations are presented in Figure 3. Since the assumption of constant moisture content would minimize convection and evaporation effects in the soil, this case approximates one of pure conduction with convection at the soil surface. Using Laplace's equation for conduction, an analytical solution was obtained (see Appendix II) and the results are presented in Figure 4. The differences between Figures 3 and 4 are explained by the fact that the heat transfer corresponding to evaporation at the surface has been neglected in obtaining the results of Figure 4. With this exception, the computer results are in good agreement with the exact results. The agreement between the calculated and experimental results of Figures 1 and 2 are deemed good enough to assume the computational approach and the differential equations valid.

The Soil Warming System

The soil warming system was simulated with the computer program for a large number of warm, porous pipes buried at uniform spacing and depth. Because the subsurface heating and irrigation system was proposed for open fields, each spacing and depth was run for two weather conditions. Weather conditions for January and August were chosen because of their extremity. In order to exemplify an approach for the optimization of the pipe spacing and depth, the weather conditions, soil properties, crop root zones, and power plant

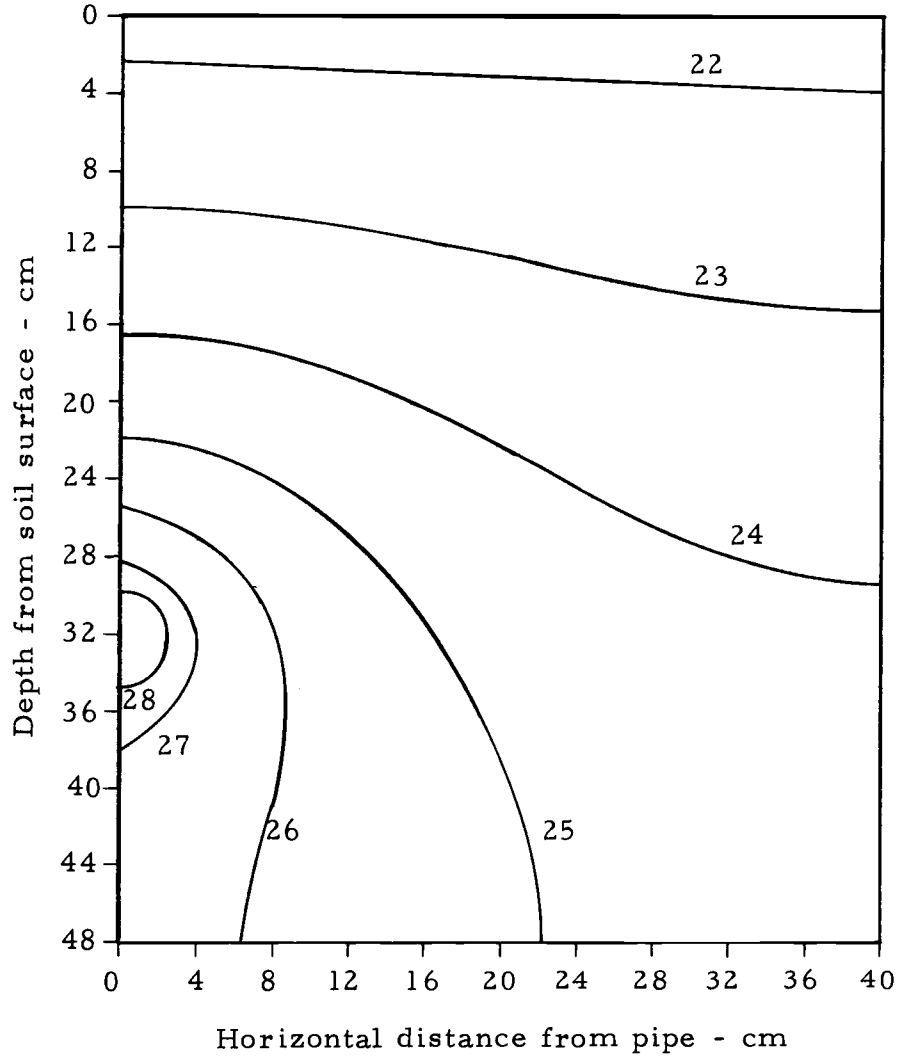

Figure 3. Calculated isotherms (°C) for constant moisture content of 0.27 cm^3/cm^3.

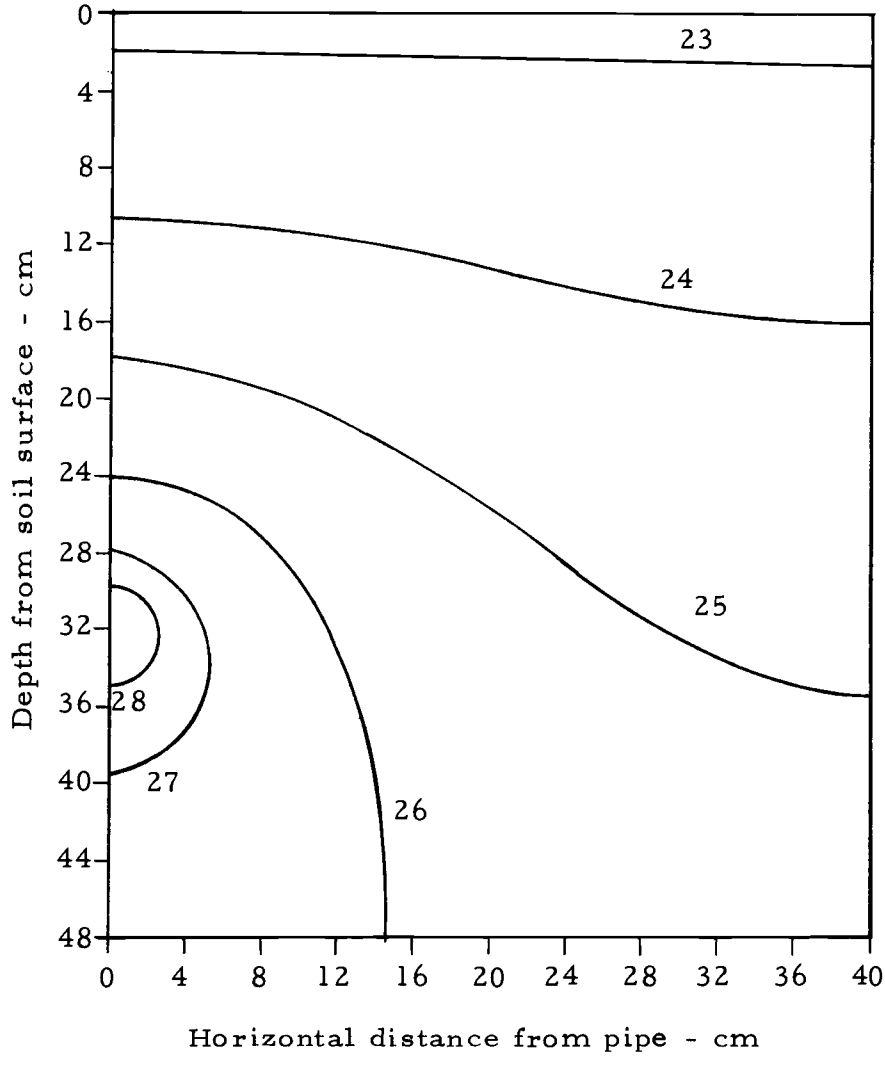

Figure 4. Isotherms for an analytical solution for constant thermal conductivity.

condenser discharge temperatures have been chosen to represent one particular location. The location and power plant condenser discharge temperatures were chosen to be representative of Portland, Oregon and the Trojan nuclear power plant. The weather data was averaged over a ten year period to obtain typical data for each day in January and August.

In order to differentiate between the effects of the pipes and the atmospheric conditions, an initial temperature and moisture content distribution was calculated for the two months. The initial distributions were calculated using average weather conditions for each month. Using these average weather conditions, the computer program was run until the temperatures and moisture contents approached steady values. No attempt was made to reach steady-state because a great many iterations would be required. The initial temperatures and moisture contents are presented in Table 1.

Pipe spacings of 140, 280, and 560 cm were selected. For the 140 and 280 cm pipe spacings, the node width was chosen to be 10.0 cm. For the 560 cm pipe spacing a node width of 20 cm was used. The node heights were 10.0 cm for the upper 200 cm and 50 cm below 200 cm. The time step employed was one day. A new daily weather condition was used for each time step and 31 time steps were used to simulate one month of operation of the heating and irrigation system.

Table 1. Initial temperature and moisture content distributions.

Depth	January		August		Depth	January	August
	T*	θ**	T	θ		T	T
0	4.2	.25	20.4	.15	250	14.7	16.9
10	4.9	.25	20.2	.18	300	14.9	16.6
20	5.5	.26	20.1	.20	350	15.1	16.2
30	6.1	.26	20.0	.21	400	15.3	15.9
40	6.7	.27	19.9	.21	450	15.4	15.6
50	7.3	.28	19.8	.24	500	15.4	15.3
60	7.9	.29	19.7	.26	550	15.3	15.1
70	8.4	.30	19.5	.28	600	15.3	14.9
80	9.0	.31	19.4	.30	650	15.2	14.7
90	9.5	.32	19.3	31	700	15.0	14.5
100	10.0	.33	19.1	.33	750	14.9	14.3
110	10.5	.35	19.0	.34	800	14.7	14.1
120	11.0	.36	18.8	.36	850	14.5	13.9
130	11.5	.37	18.7	.37	900	14.3	13.7
140	11.9	.38	18.5	.38	950	14.1	13.5
150	12.4	.39	18.3	.39	1000	14.0	13.2
160	12.8	.40	18.1	.40	1050	13.8	13.0
170	13.2	41	17.9	.41	1100	13.6	12.8
180	13.6	.42	17.6	.42	1150	13.4	12.5
190	13.9	.43	17.4	.43	1200	13.1	12.3
200	14.3	.44	17.1	.44	1250	12.8	12.0
					1300	12.3	11.6
					1350	11.5	11.0

*T denotes temperatures - °C.
**θ denotes moisture content cm^3/cm^3. Below 200 cm $\theta = .45\ cm^3/cm^3$.

The pipe temperature was chosen to represent condenser cooling water outlet temperatures with an allowance for heat loss. The pipe temperatures were 29 C for January and 41 C for August. The soil properties used were those of a sandy soil common in the Portland area. Since the system is intended to serve as a means of irrigation, the moisture content of the soil adjacent to the pipe was assumed to be

constant at 0.44 cm^3/cm^3, which is slightly lower than the saturation moisture content of 0.45 cm^3/cm^3.

Using the nodal sizes, time step, weather conditions, soil properties and initial distributions mentioned above, the computer program was run representing 31 days of operation of the soil warming system for the months of January and August. Temperature and moisture content distributions were obtained for the three pipe spacings mentioned above and for pipe depths of 50 and 100 cm. The temperature and moisture content distributions after 31 days of operation as obtained from the computer program are presented in Figures 5 through 24.

Figure 25 presents the results of the equation of Kendricks and Havens for a pipe spacing of 280 cm and a pipe depth of 100 cm. The pipe temperature was 41 C and the soil surface temperature was 19.7 C. The pipe radius was assumed to be 1.0 cm. The pipe spacing, depth and temperature were the same as for Figure 9, while the soil surface temperature was approximately the same. While the temperatures for Figure 9 were not for steady-state, the effect of assuming constant thermal conductivity and neglecting convective effects in the analysis of Kendricks and Havens can be seen by comparing the location of the 34 C isotherm. The location of an isotherm is closer to the pipe during the transient period than during the steady-state period for transient analyses. The fact that the 34 C isotherm

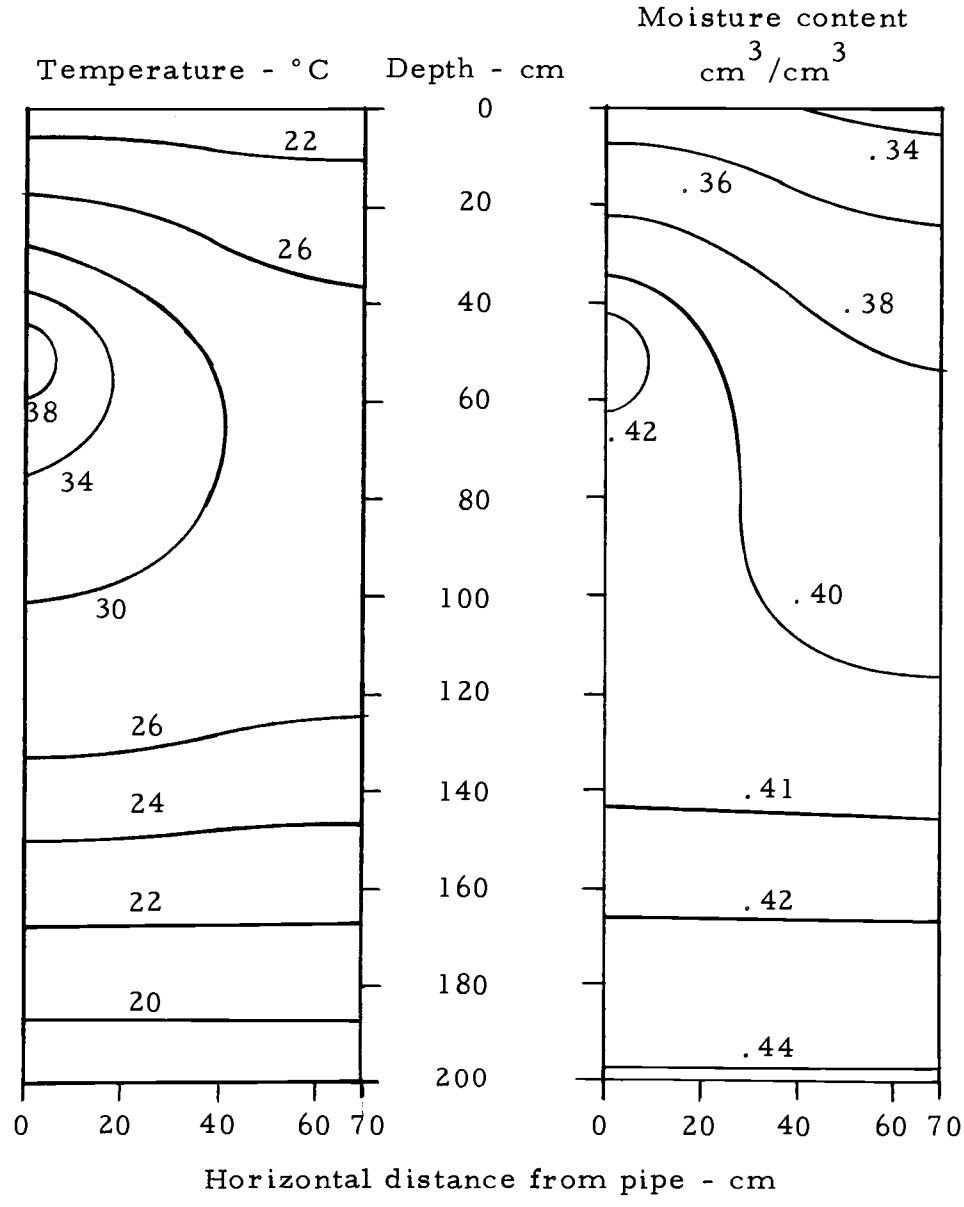

Figure 5. Temperature and moisture content distributions for August conditions, pipe spacing of 140 cm and pipe depth of 50 cm.

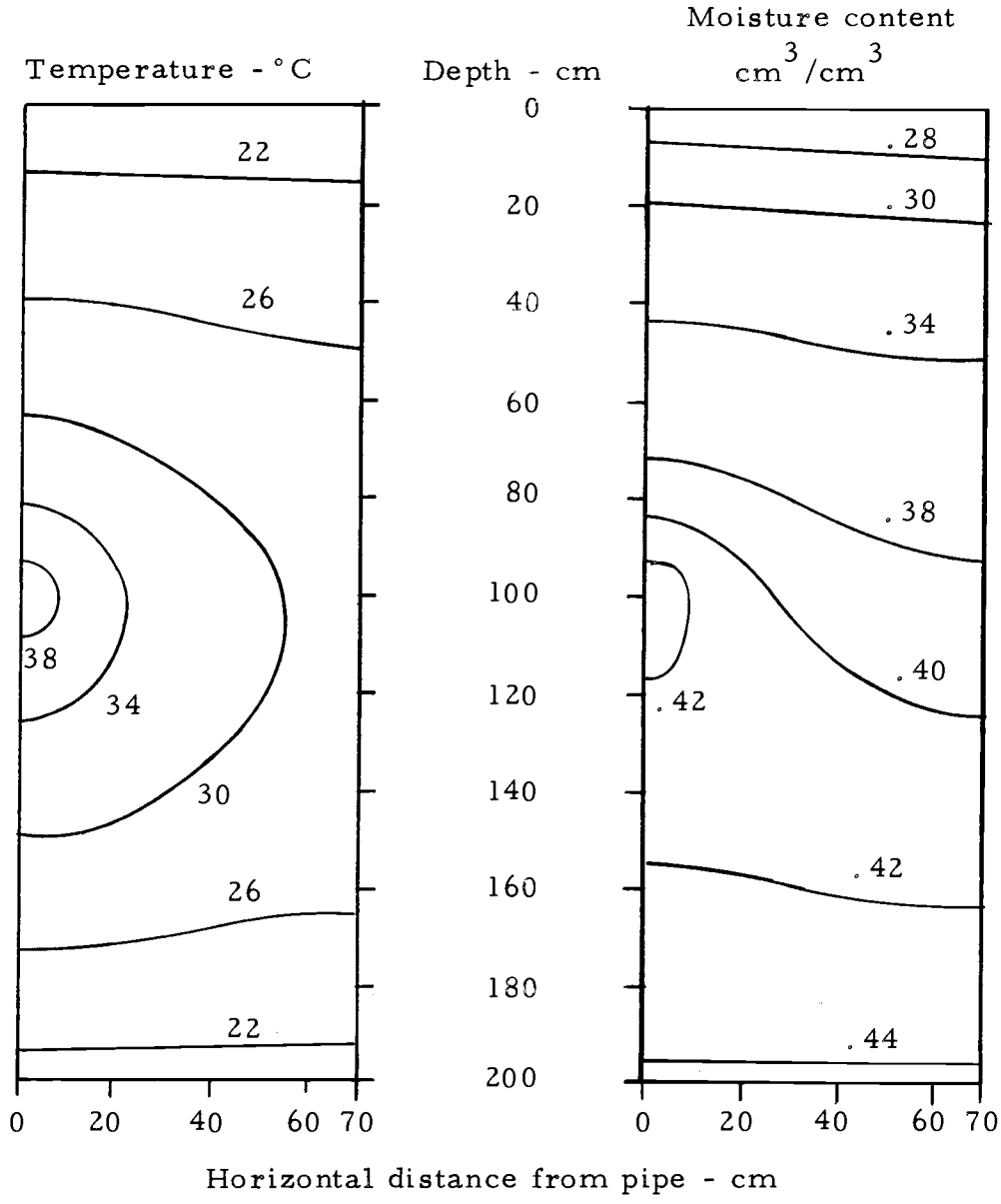

Figure 6. Temperature and moisture content distributions for August conditions, pipe spacing of 140 cm and pipe depth of 100 cm.

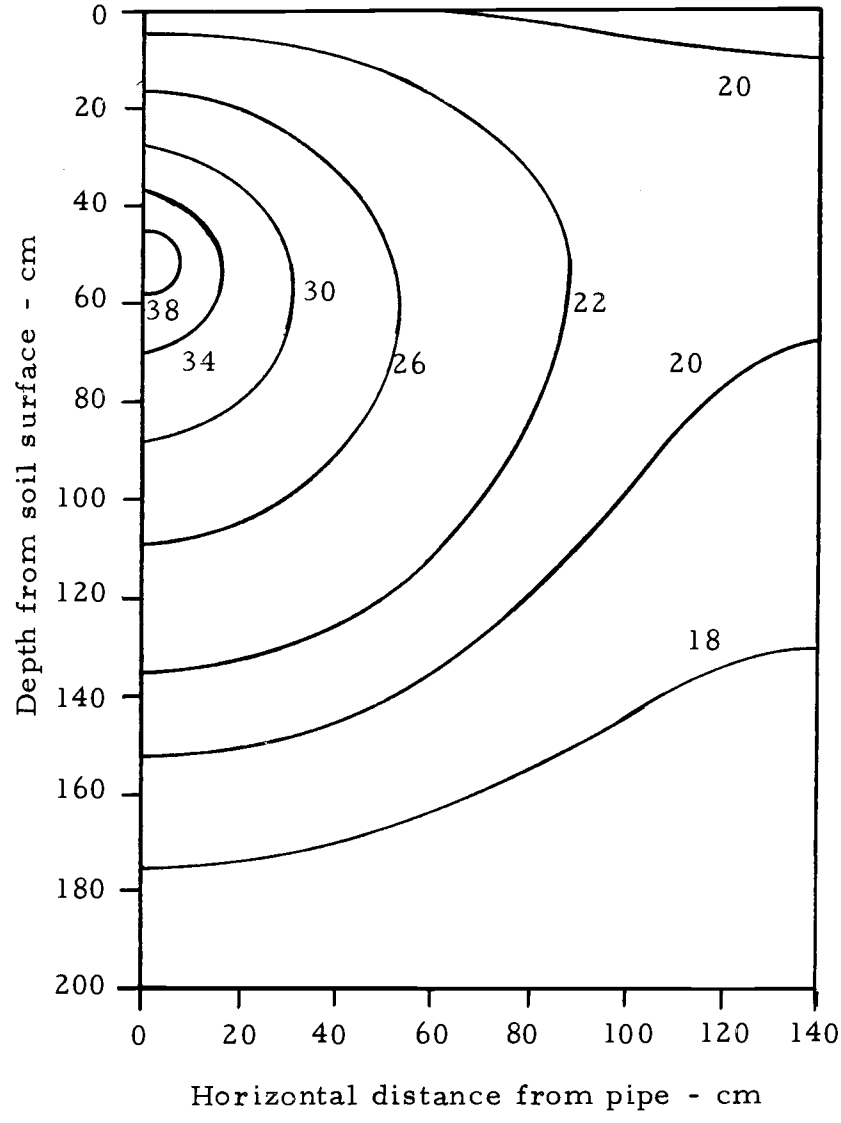

Figure 7. Isotherms (°C) for August conditions, pipe spacing of 280 cm and pipe depth of 50 cm.

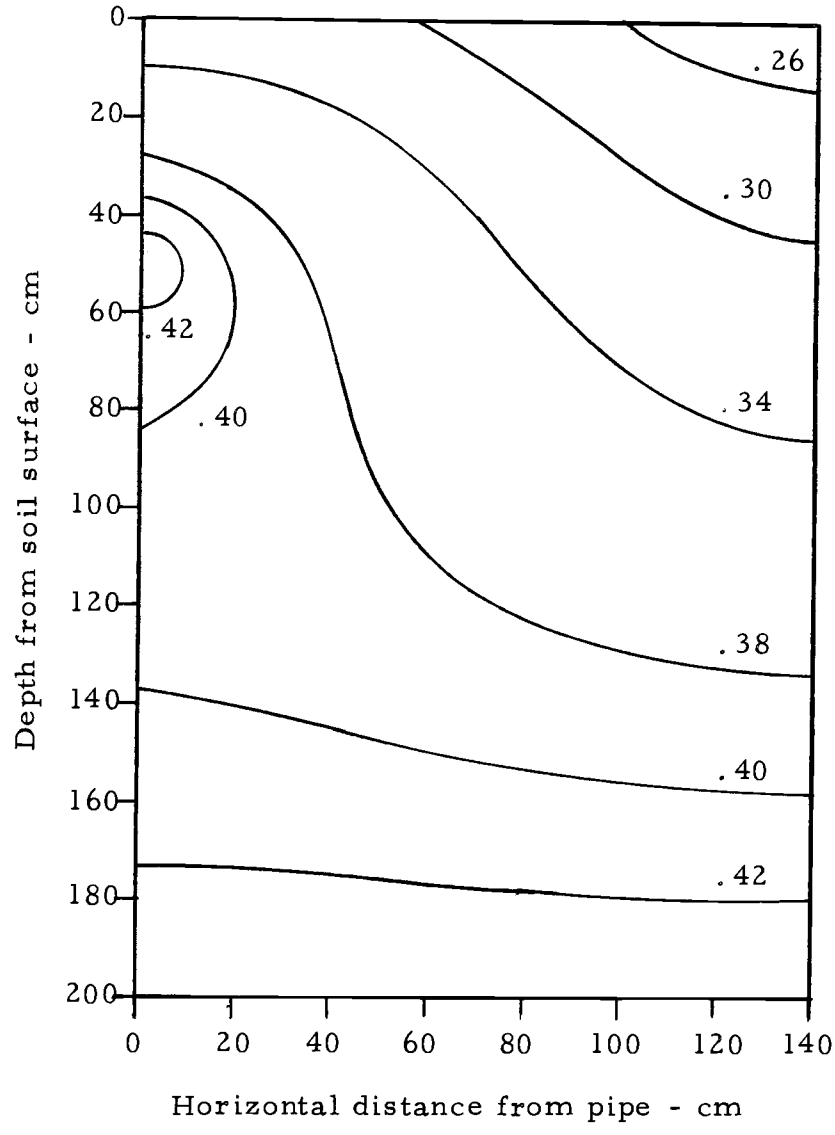

Figure 8. Moisture content distribution (cm^3/cm^3) for August conditions, pipe spacing of 280 cm and pipe depth of 50 cm.

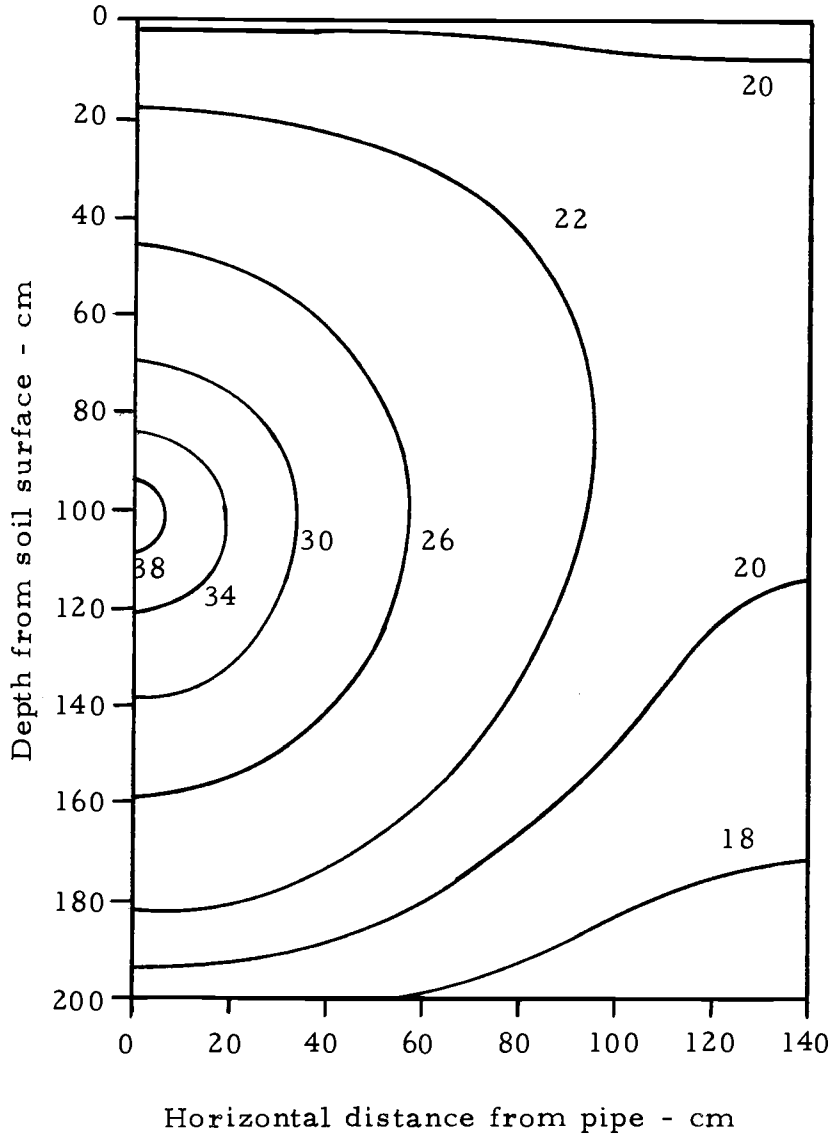

Figure 9. Isotherms (°C) for August conditions, pipe spacing of 280 cm and pipe depth of 100 cm.

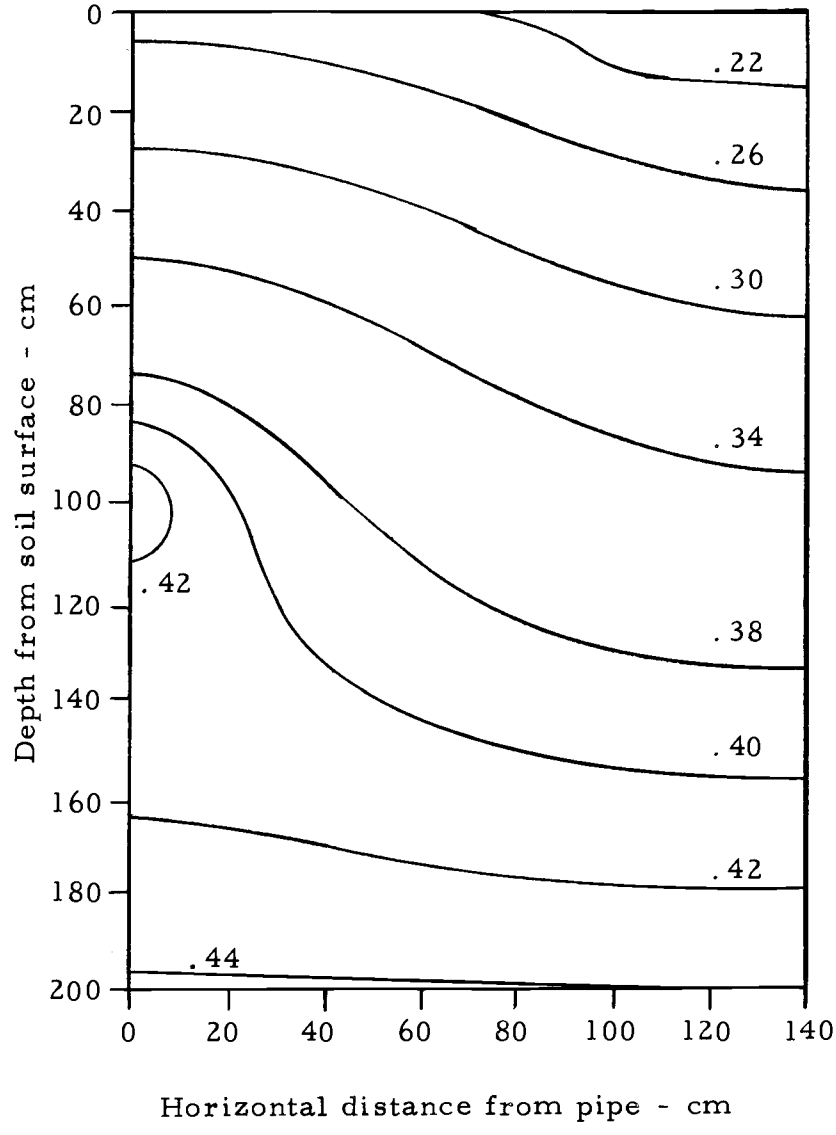

Figure 10. Moisture content distribution (cm^3/cm^3) for August conditions, pipe spacing of 280 cm and pipe depth of 100 cm.

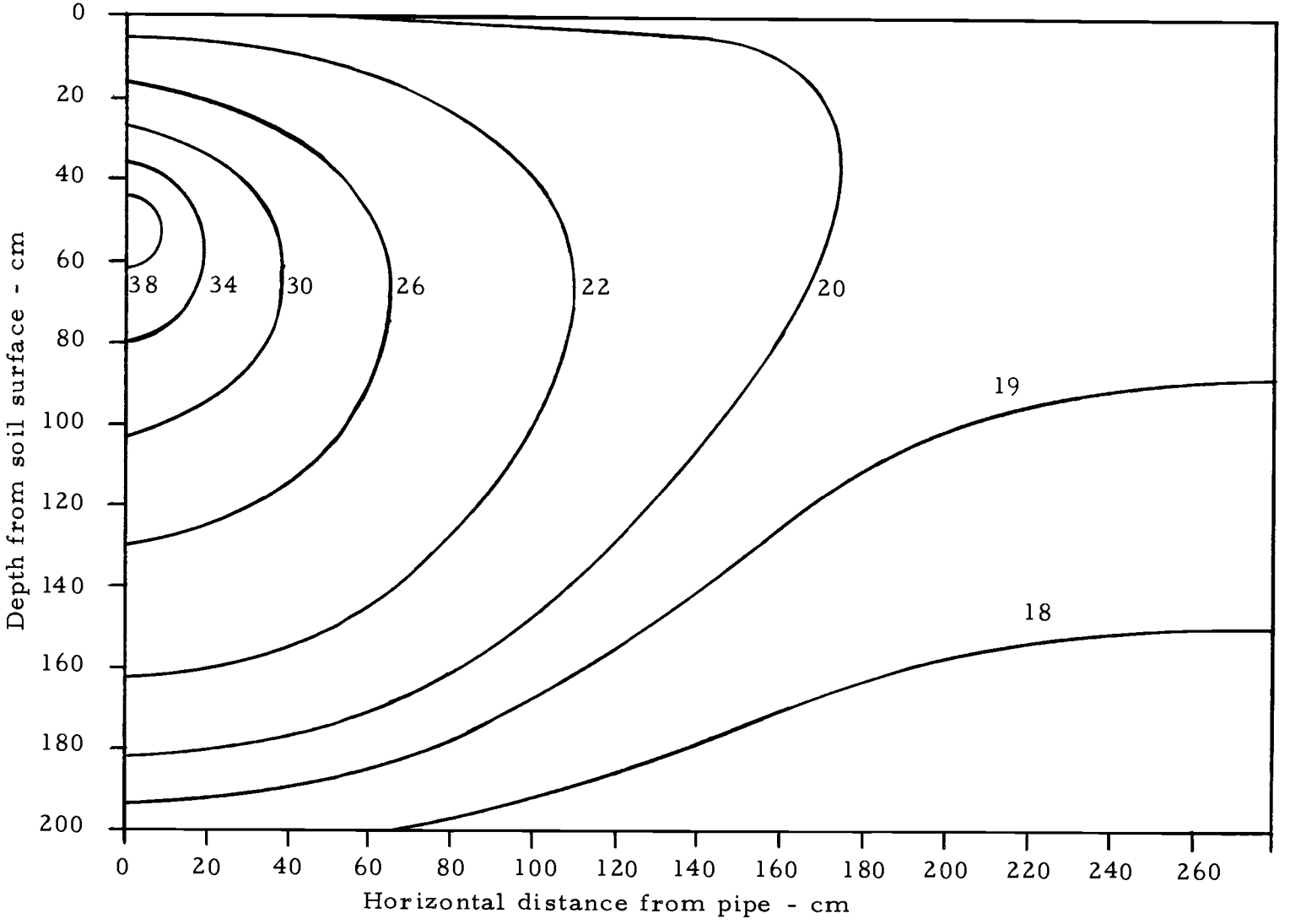

Figure 11. Isotherms (°C) for August conditions, pipe spacing of 560 cm and pipe depth of 50 cm.

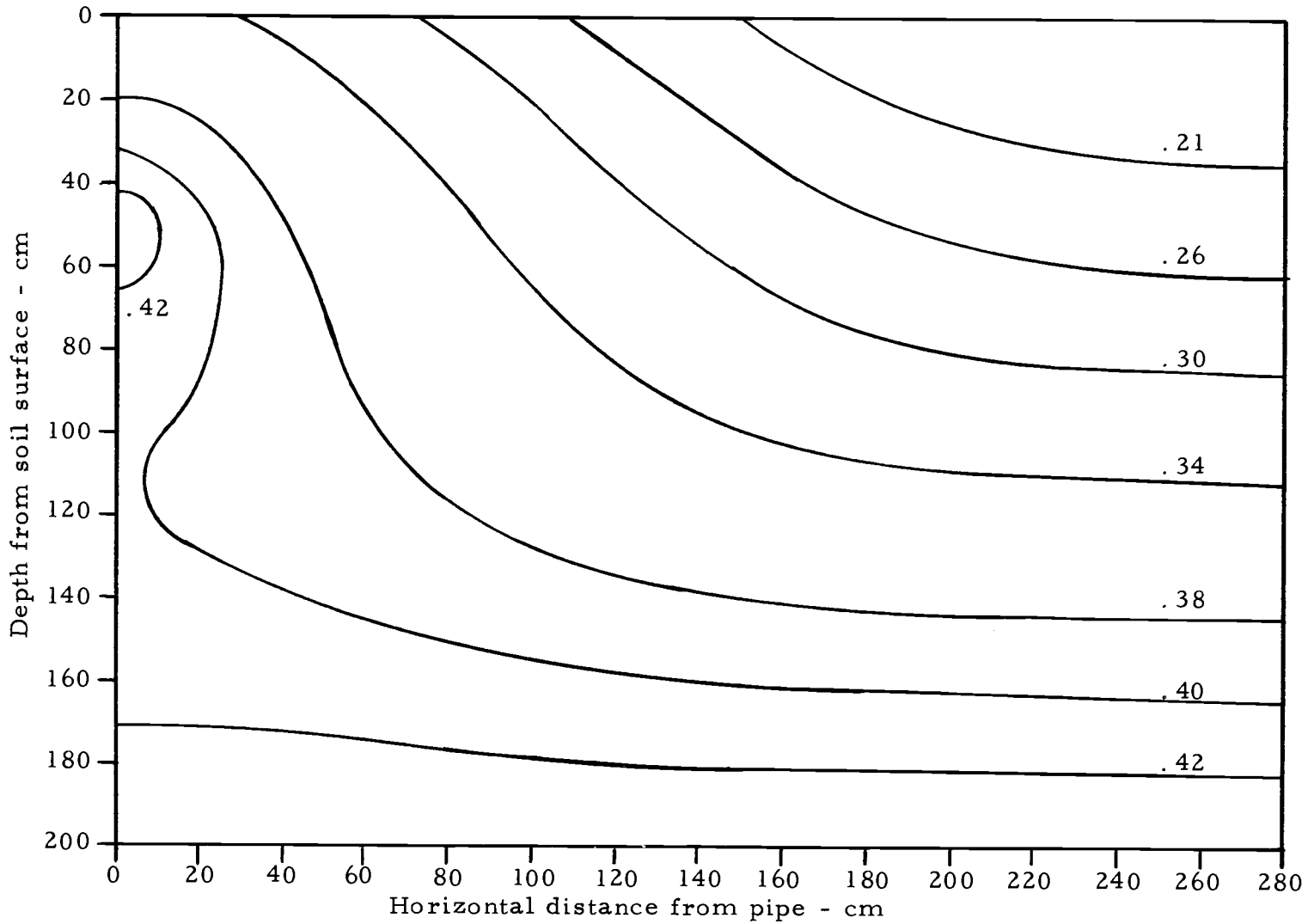

Figure 12. Moisture content distribution (cm^3/cm^3) for August conditions, pipe spacing of 560 cm and pipe depth of 50 cm.

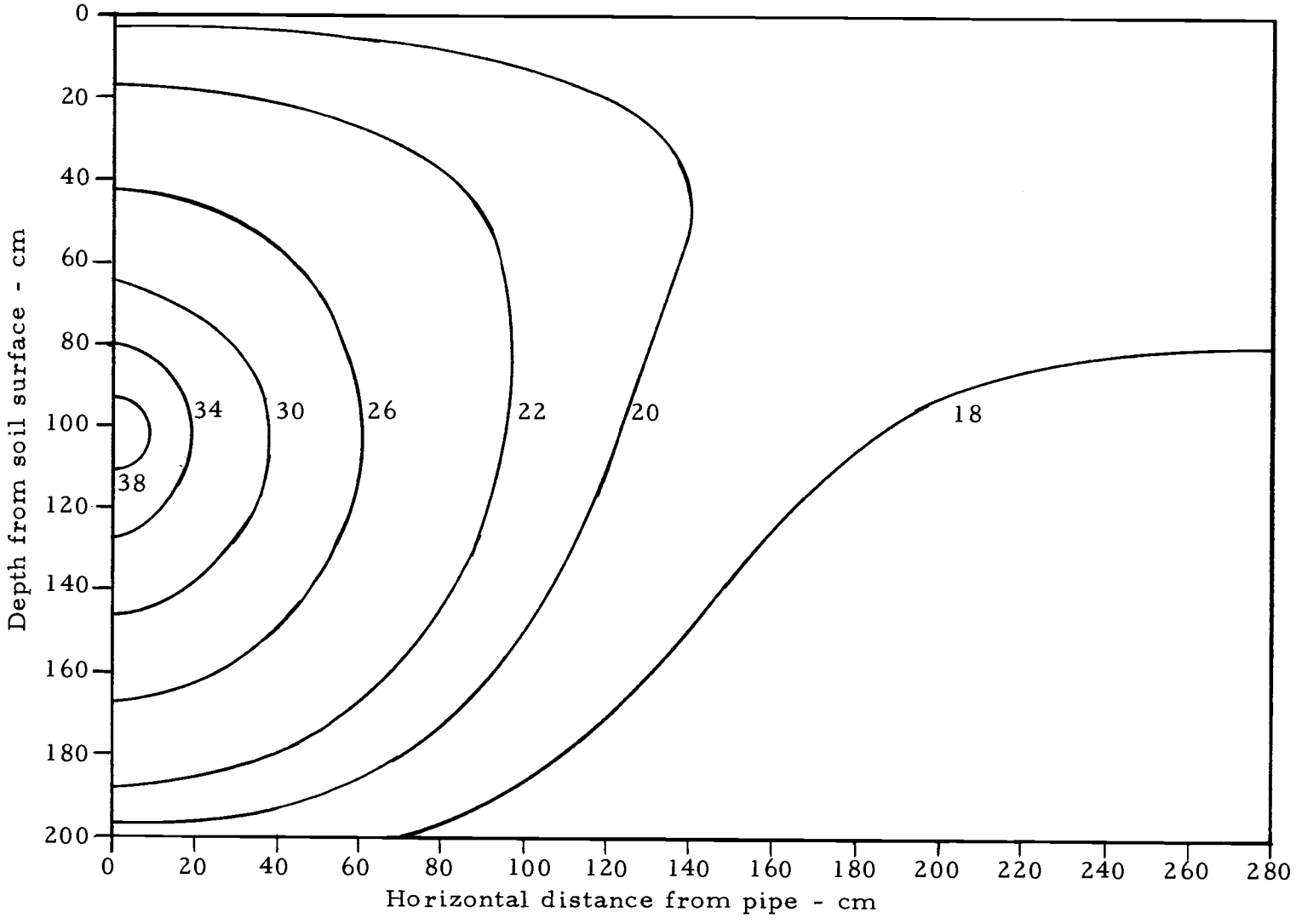

Figure 13. Isotherms (°C) for August conditions, pipe spacing of 560 cm and pipe depth of 100 cm.

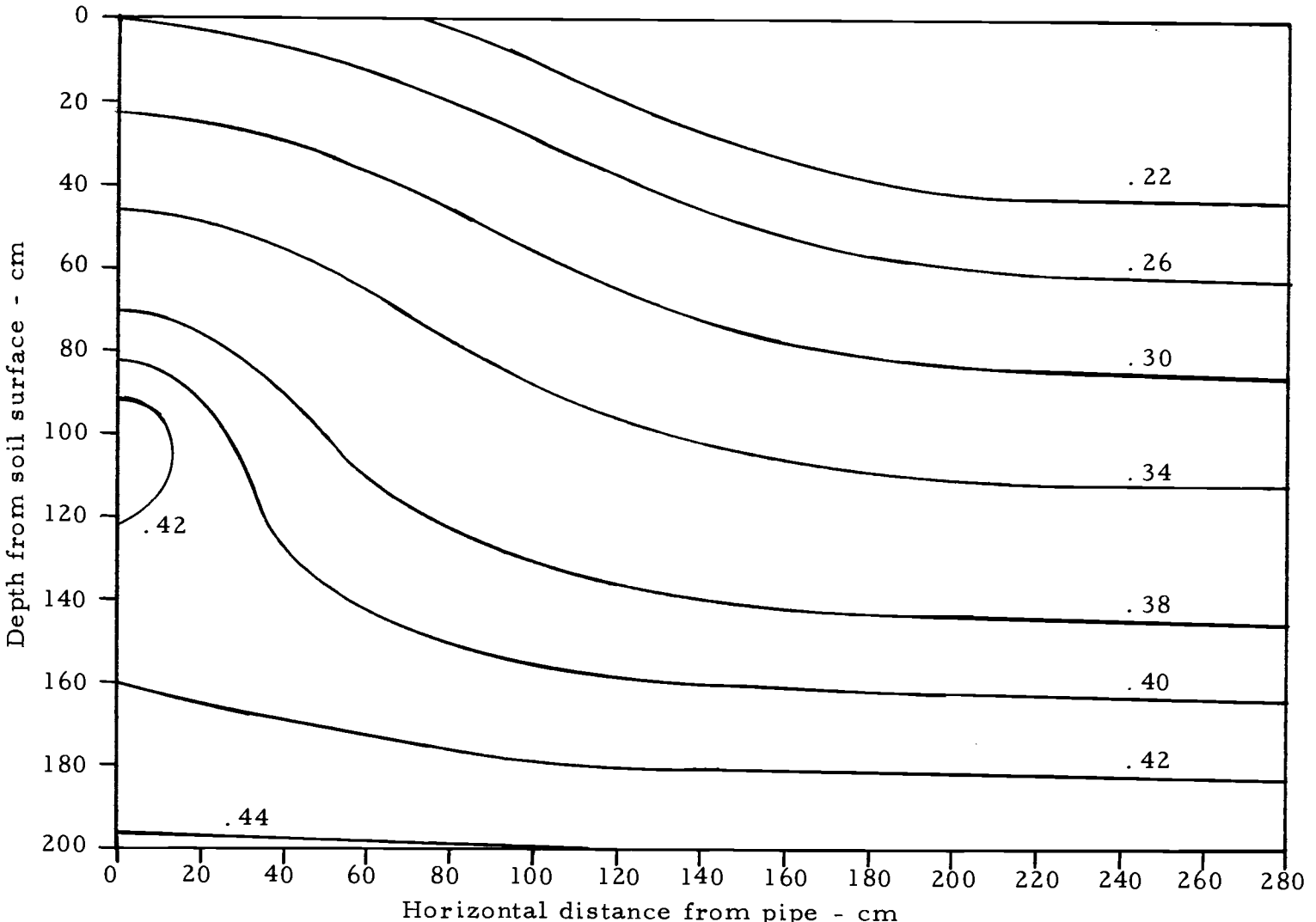

Figure 14. Moisture content distribution (cm^3/cm^3) for August conditions, pipe spacing of 560 cm and pipe depth of 100 cm.

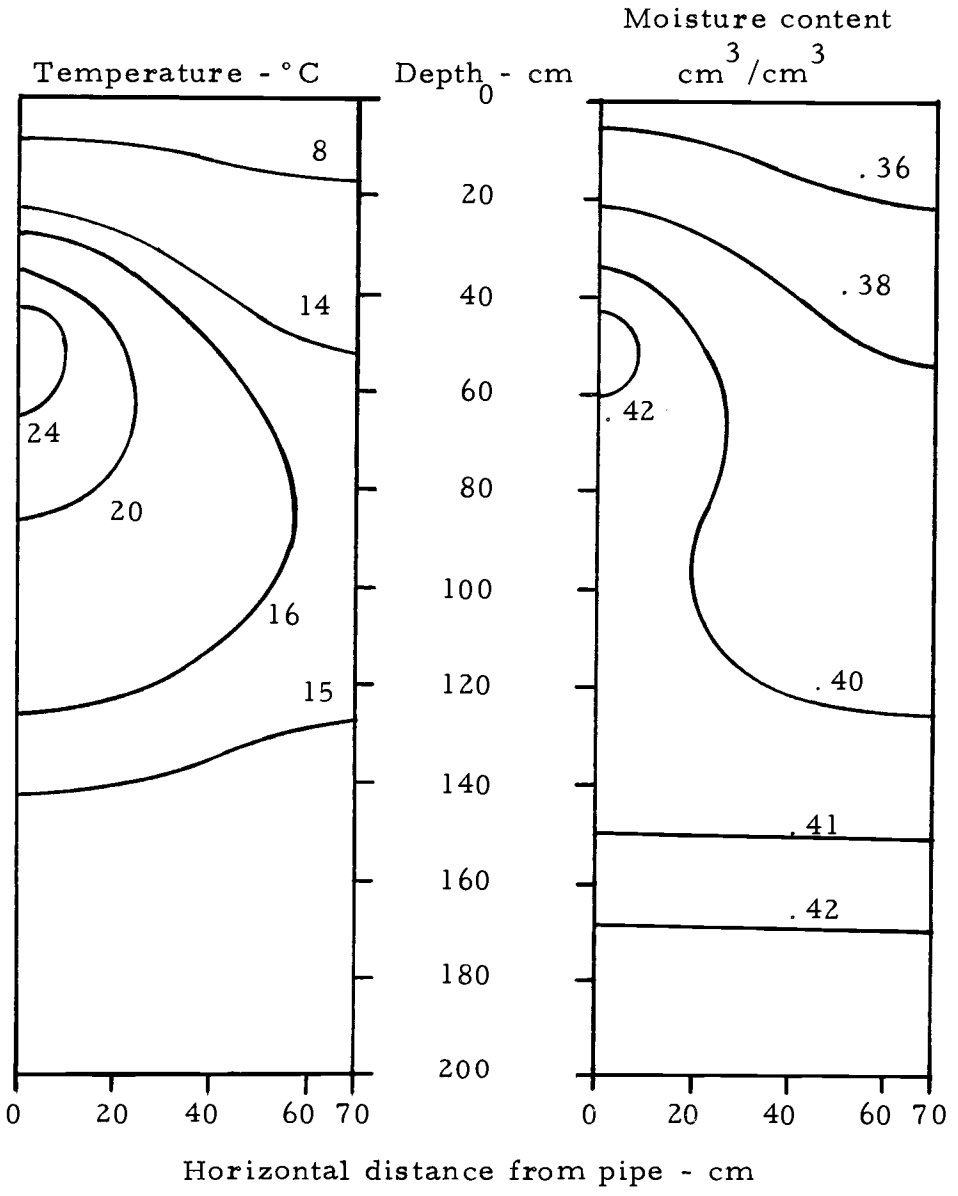

Figure 15. Temperature and moisture content distributions for January conditions, pipe spacing of 140 cm and pipe depth of 50 cm.

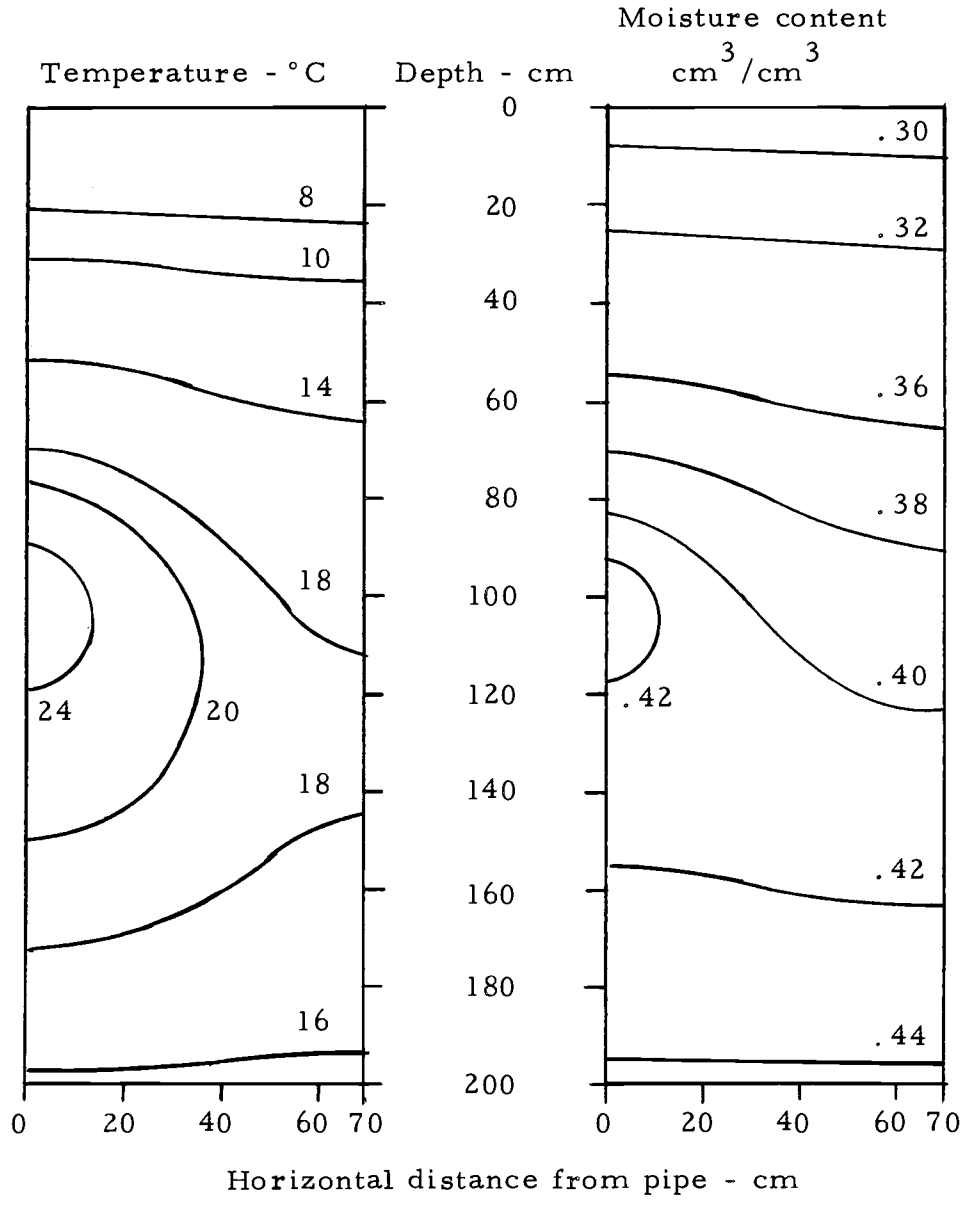

Figure 16. Temperature and moisture content distributions for January, pipe spacing of 140 cm and pipe depth of 100 cm.

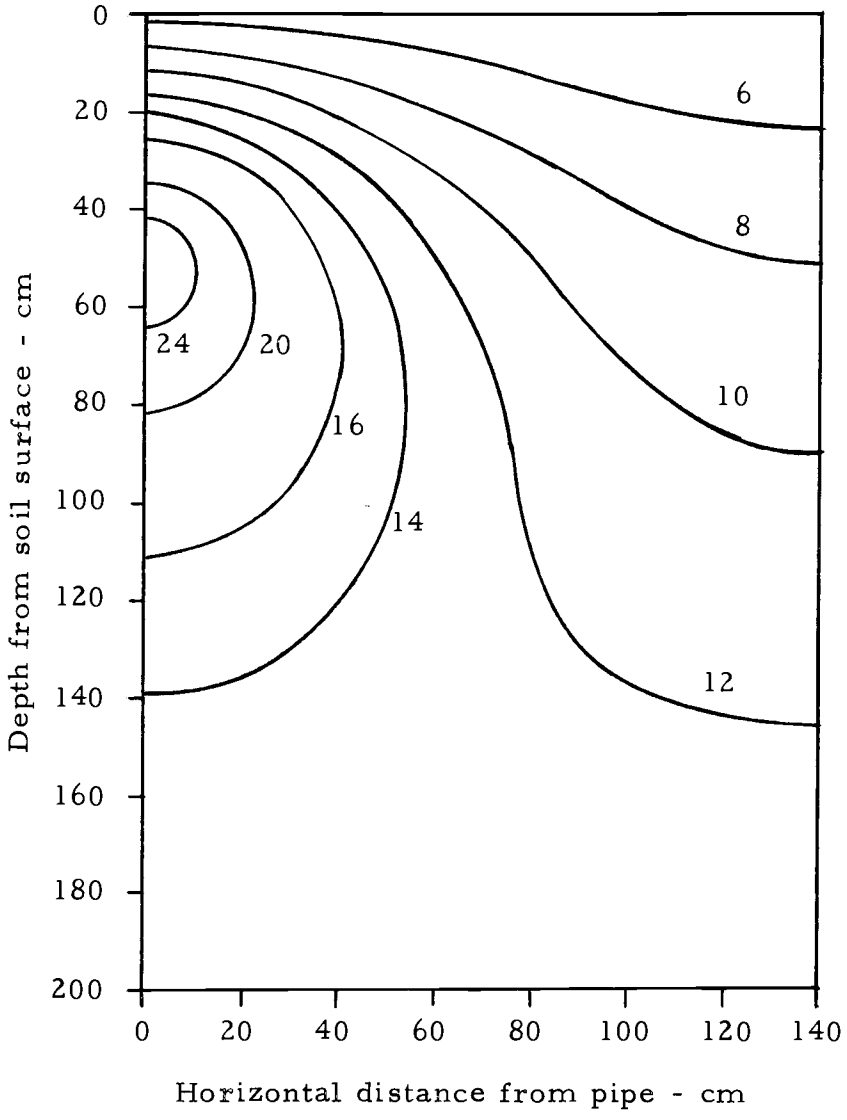

Figure 17. Isotherms (°C) for January conditions, pipe spacing of 280 cm, and pipe depth of 50 cm.

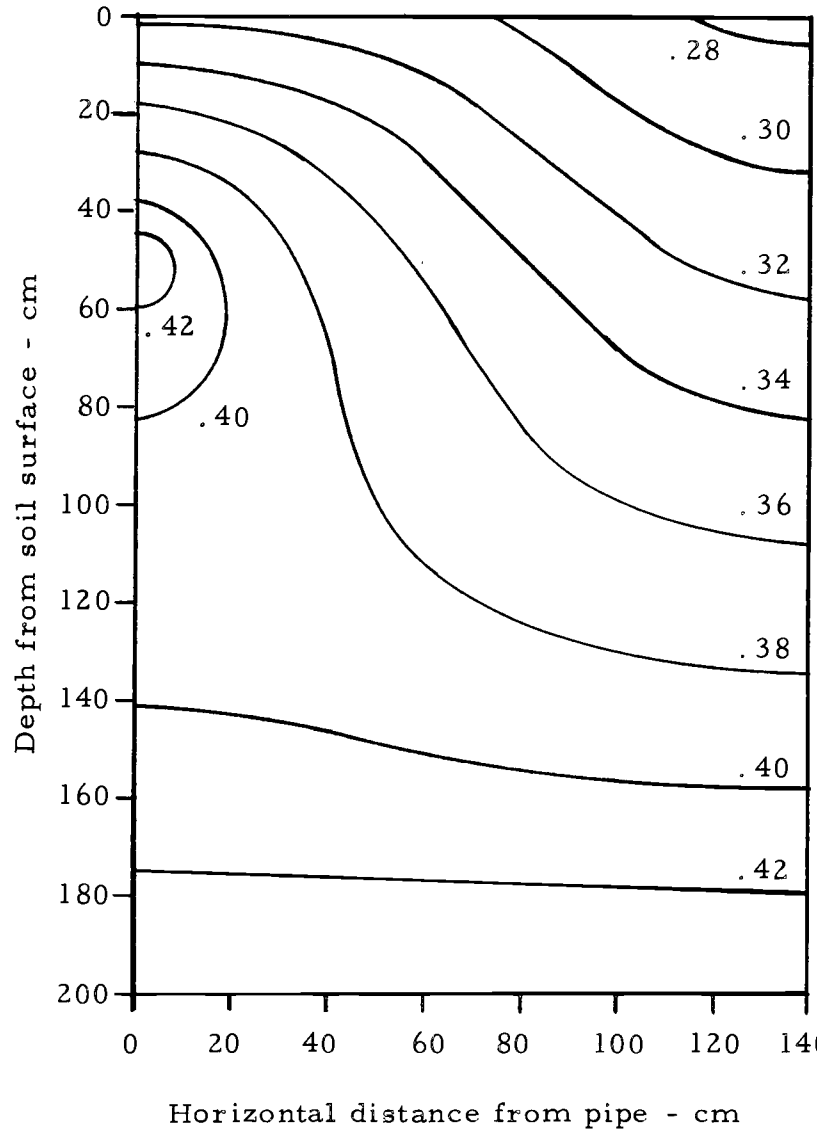

Figure 18. Moisture content distribution (cm^3/cm^3) for January, pipe spacing of 280 cm and pipe depth of 50 cm.

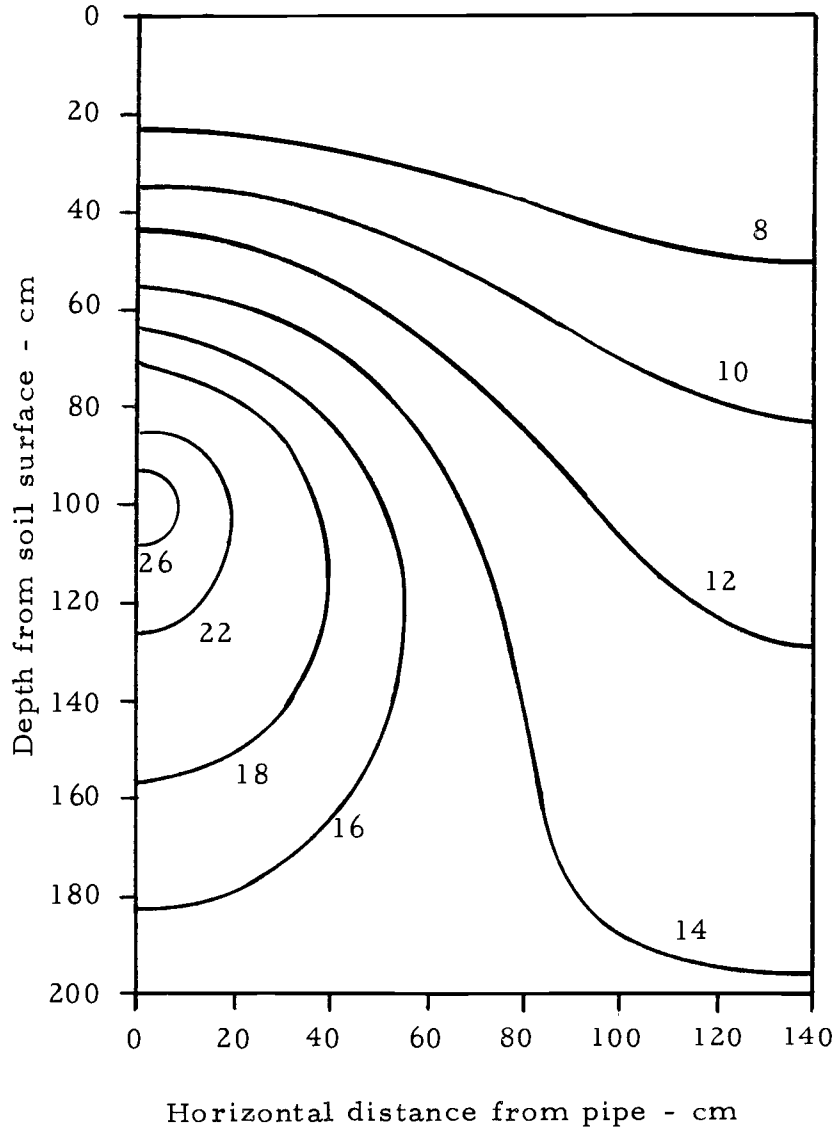

Figure 19. Isotherms (°C) for January conditions, pipe spacing of 280 cm and pipe depth of 100 cm.

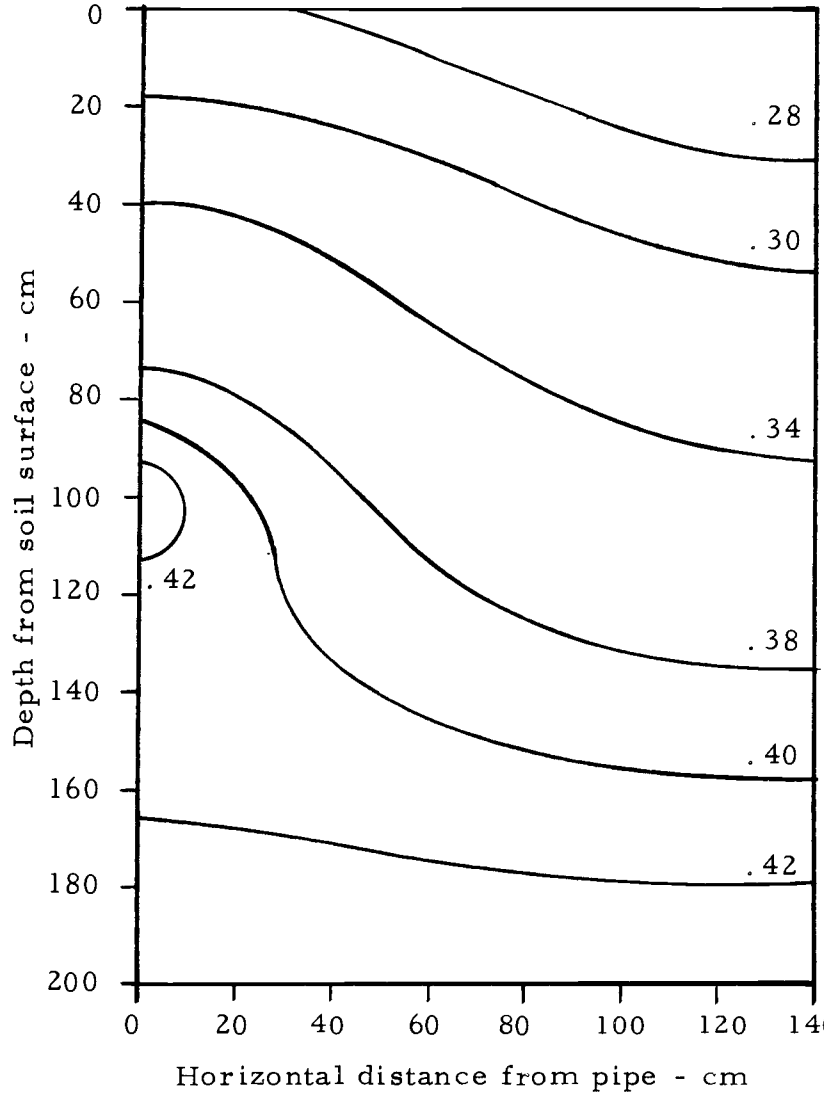

Figure 20. Moisture content distribution (cm^3/cm^3) for January, pipe spacing of 280 cm and pipe depth of 100 cm.

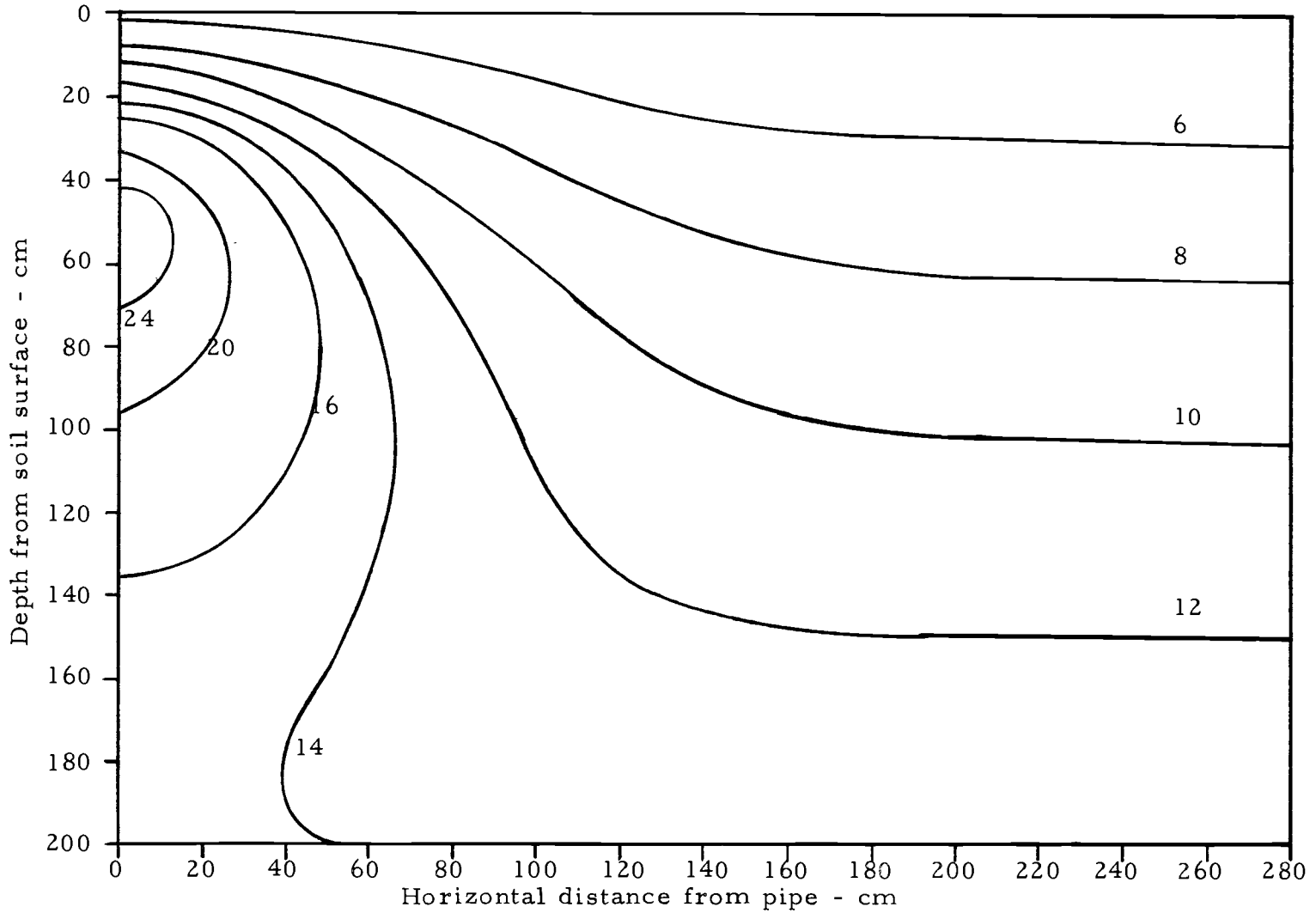

Figure 21. Isotherms (°C) for January conditions, pipe spacing of 560 cm and pipe depth of 50 cm.

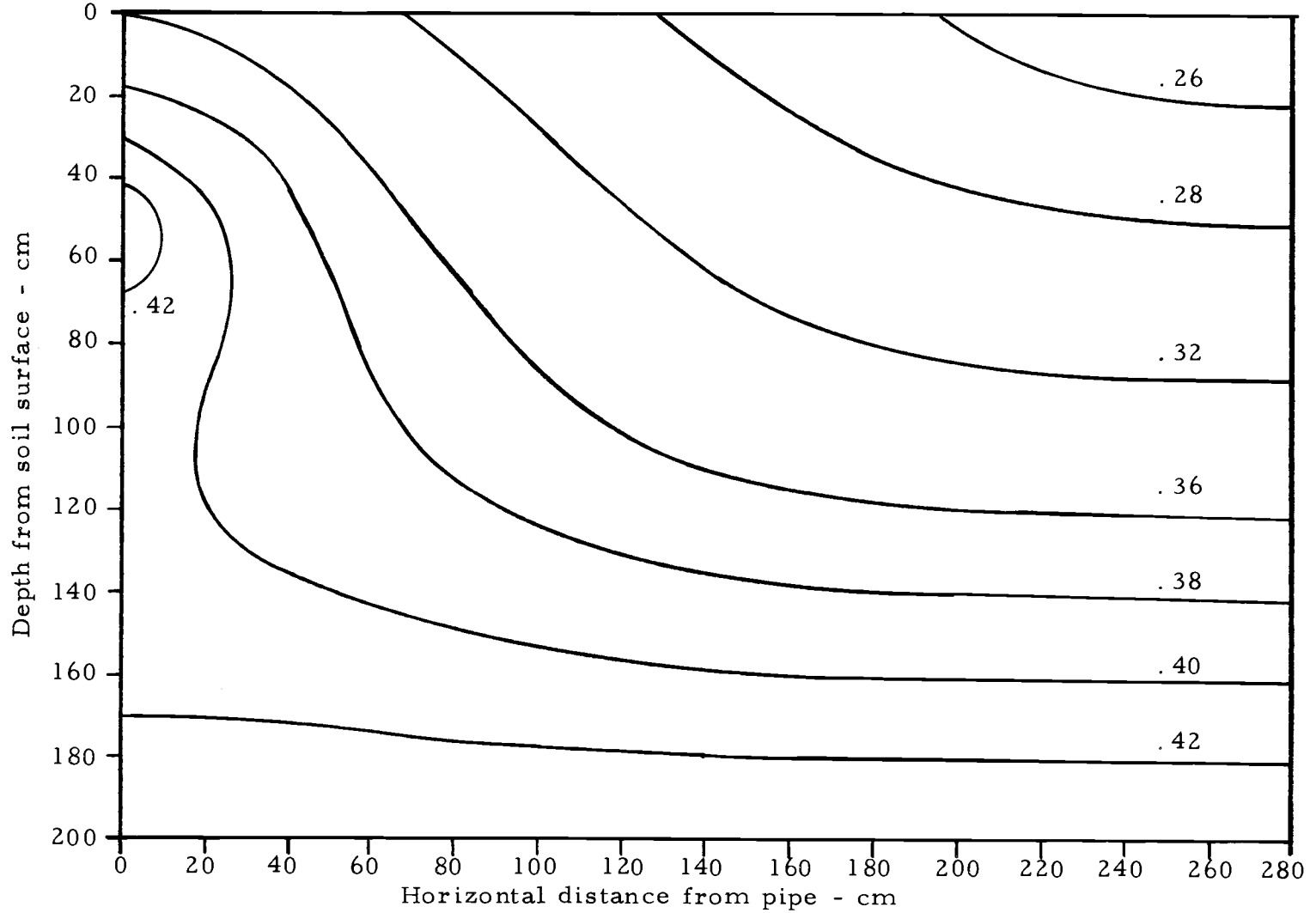

Figure 22. Moisture content distribution (cm^3/cm^3) for January conditions, pipe spacing of 560 cm and pipe depth of 50 cm.

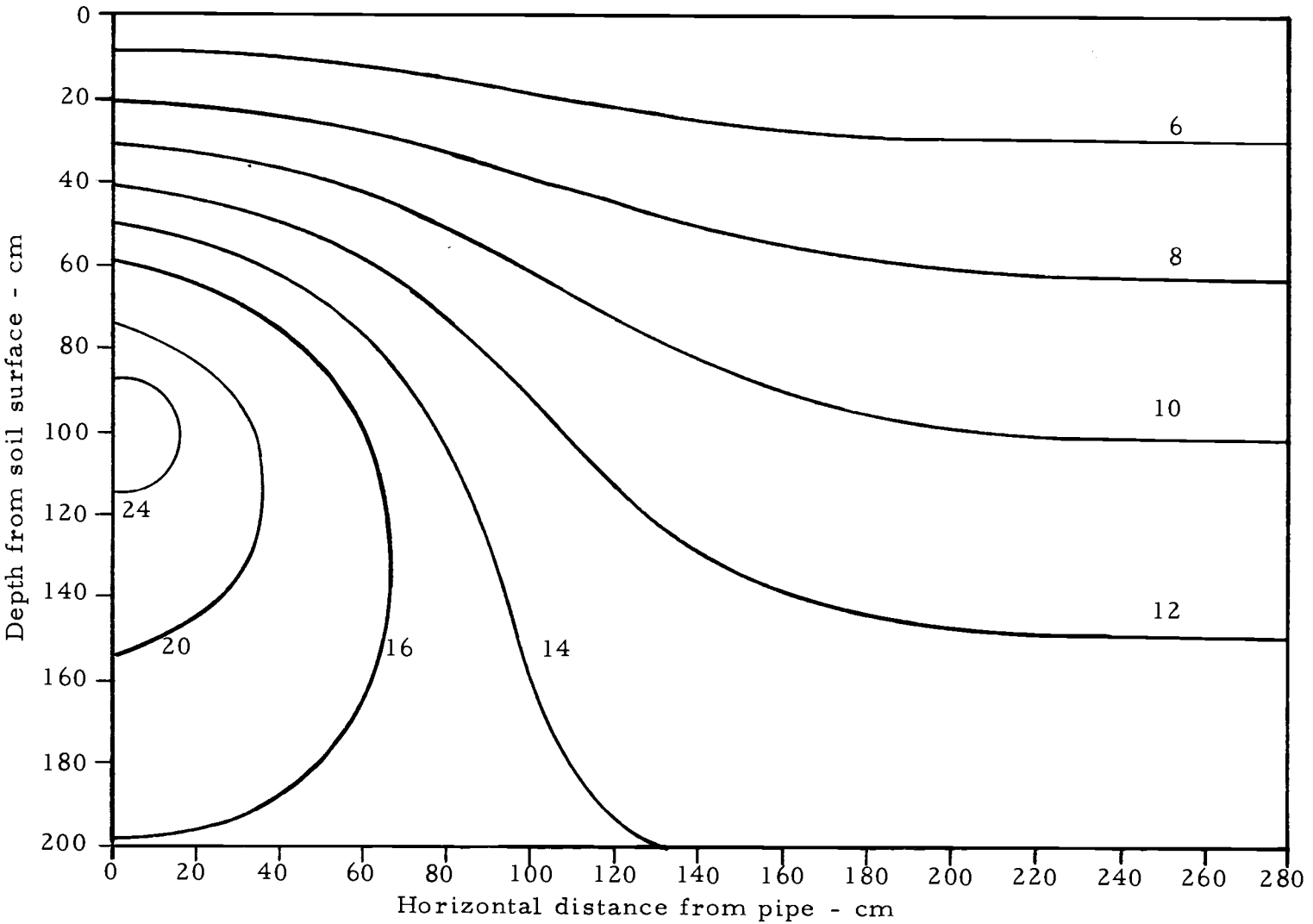

Figure 23. Isotherms (°C) for January conditions, pipe spacing of 560 cm and pipe depth of 100 cm.

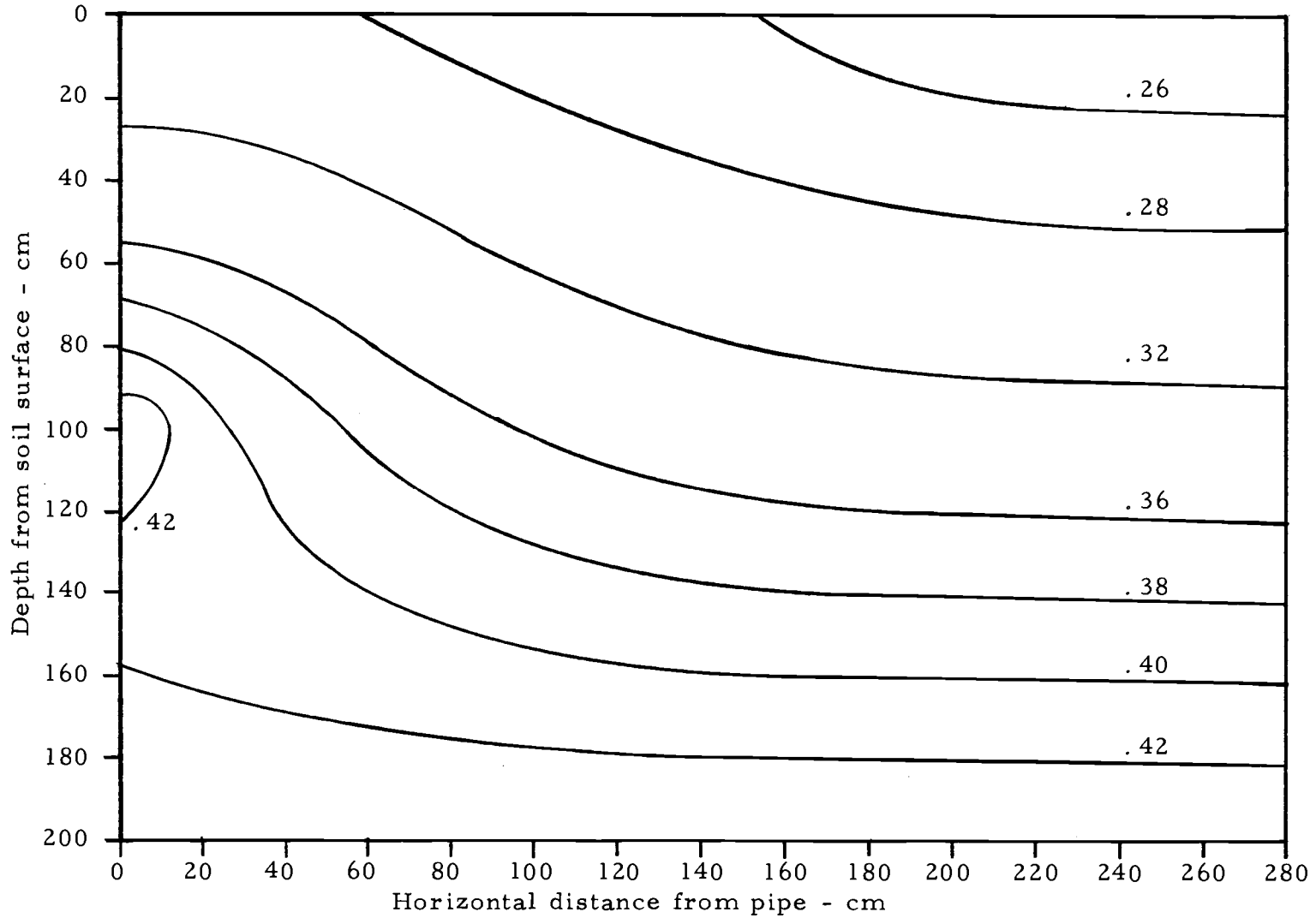

Figure 24. Moisture content distribution (cm^3/cm^3) for January conditions, pipe spacing of 560 cm and pipe depth of 100 cm.

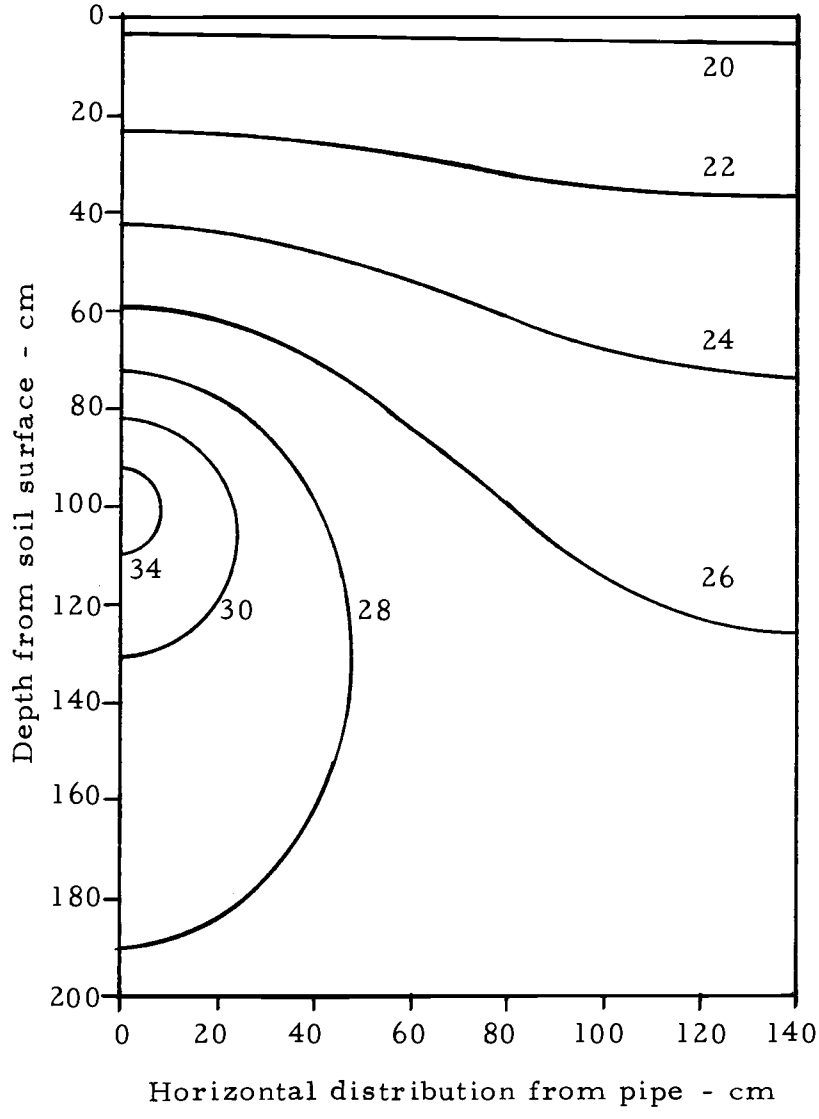

Figure 25. Results of the equation of Kendricks and Havens for a pipe spacing of 280 cm and pipe depth of 100 cm, presented as isotherms (°C).

is farther from the pipe in Figure 9 (the analysis of the present investigation) than in Figure 25 (the analysis of Kendricks and Havens) is due to the error induced by assumption of constant thermal conductivity and of neglecting the convective effects in the analysis of Kendricks and Havens. The analysis of Kendricks and Havens has the additional disadvantage that the surface temperature of the soil must be specified. For the analysis of the present investigation, the soil surface temperature was less than 20 C in August, while the atmospheric temperature was about 31 C. The soil surface temperature may then be 10 C less than the atmospheric temperature. Since the analysis of Kendricks and Havens provides no means for obtaining the soil surface temperature, errors of the order of 10 C would be expected.

In the previous cases only parallel flow through the pipes was considered. An alternative arrangement would be to circulate the water in opposite directions in alternating pipes. To demonstrate the capability of the computer program to model the case of counterflow through alternating pipes, the computer program was run for the case of alternating pipes at 41 C and 31 C. The weather data and initial temperatures and moisture contents were those previously used for the month of August. The moisture content of the soil adjacent to the pipes was 0.44 cm^3/cm^3. The pipe depth was 100 cm and the node heights and time step were the same as for the previous cases. For

this case calculations were carried out for 50 time steps. The temperature and moisture content distributions are presented in Figures 26 and 27.

Optimization Criteria

Two factors influencing plant growth are temperature and moisture content. Low temperatures may retard plant growth, while plant growth increases as the temperature increases until the wilting temperature is reached. The percent of the root zone in excess of 24 C was chosen as a possible optimization parameter because 24 C was the lower of the optimum soil temperatures (14). Another optimization parameter calculated was the average increase in temperature in the root zone above the initial temperature. This criteria is suggested because it is representative of the heating effect of the soil warming and irrigation system. A third optimization criteria which was calculated was the average increase in moisture content in the root zone above the initial moisture content distribution. These three optimization criteria were calculated for the final temperature and moisture content distributions obtained from the use of the computer program for root zones of 100 cm and 200 cm depth. The three criteria are presented in Table 2.

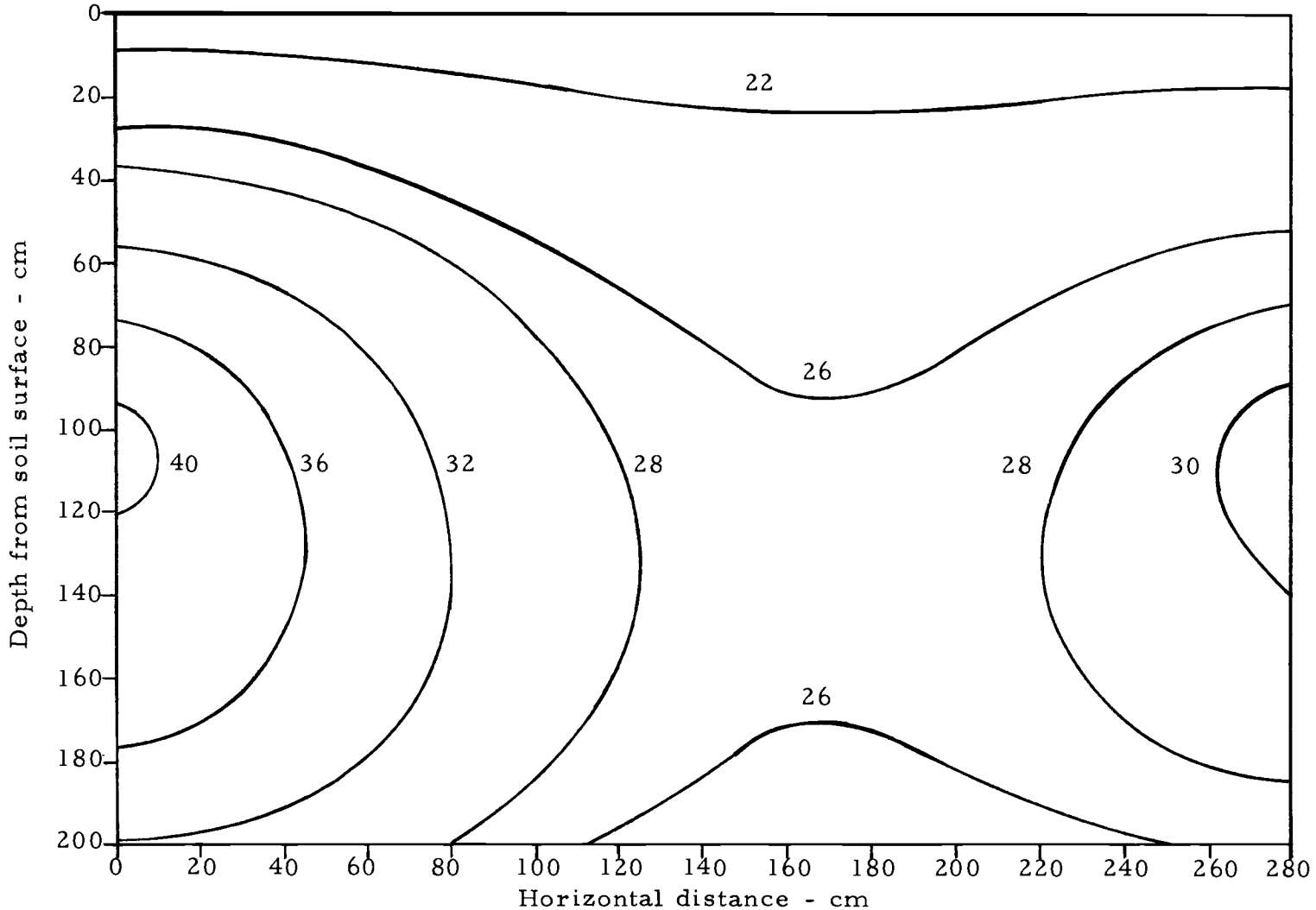

Figure 26. Isotherms (°C) for August conditions, pipe spacing of 280 cm and pipe depths of 100 cm. The left pipe temperature was 41°C while the right was 31°C.

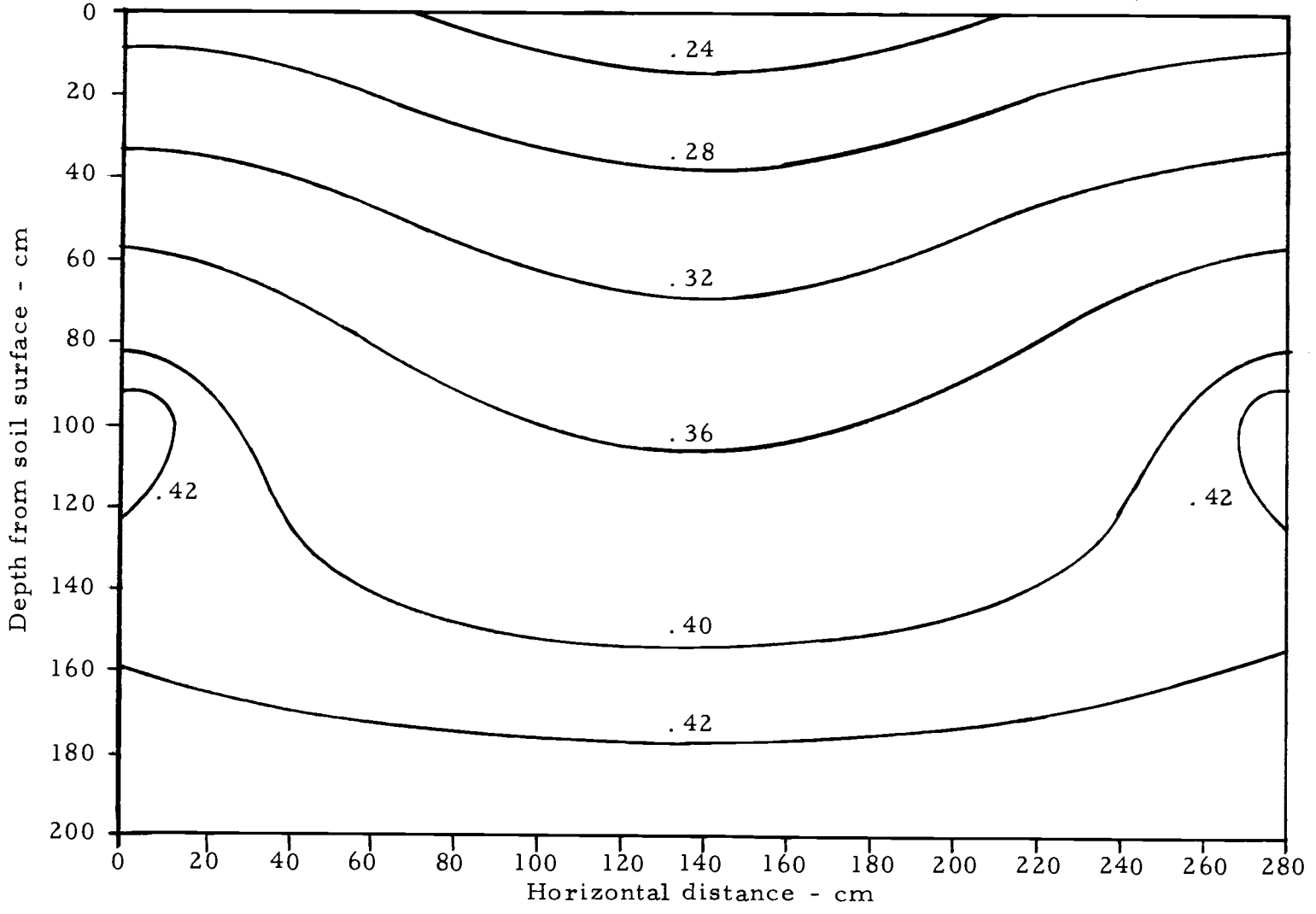

Figure 27. Moisture content distribution (cm^3/cm^3) for August conditions, pipe spacing of 280 cm and pipe depth of 100 cm for alternating pipes.

Table 2. Suggested optimization criteria.

Root Zone Depth	Spacing	Pipe Depth (cm) 50	Pipe Depth (cm) 100	Pipe Depth (cm) 50	Pipe Depth (cm) 100	Pipe Depth (cm) 50	Pipe Depth (cm) 100
cm	cm	Percent of Soil Above 24°C		Ave. Temp. Increase (°C)		Ave. Moisture Increase (cm^3/cm^3)	
January							
200	140	1.08	2.19	5.12	6.06	.0634	.0473
	280	0.57	0.86	2.44	2.83	.0386	.0264
	560	0.42	0.77	1.44	1.76	.0254	.0163
100	140	2.16	1.50	7.99	6.16	.104	.0673
	280	1.14	0.58	4.22	3.05	.0654	.0385
	560	0.84	0.46	2.42	1.91	.0423	.0237
August							
200	140	65.6	77.0	7.12	8.50	.0846	.0638
	280	20.7	28.2	2.31	3.76	.0569	.0397
	560	14.5	16.4	1.99	1.65	.0337	.0211
100	140	83.2	72.2	9.04	7.65	.144	.0997
	280	36.8	28.2	4.15	3.69	.101	.0640
	560	10.0	16.3	2.62	1.60	.0601	.0346

IV. CONCLUSIONS AND RECOMMENDATIONS

While the results presented in Table 2 do not alone provide an optimum spacing and depth for the pipes, several generalizations can be made. The 50 cm pipe depth provides better irrigation than the 100 cm pipe depth. This is due to the effect of gravity on the flow of water and to the drying of the upper region of the soil through evaporation at the surface. From the standpoint of irrigation then, the pipe spacing should be small and the pipe depth should be as shallow as possible. Cultivation requirements demand a depth of at least 32.0 cm.

A pipe depth of 50 cm appears to produce greater heating effects for crops with a root zone of 100 cm depth than the 100 cm pipe depth. Furthermore, for a root zone depth of 200 cm, the heating effects are not greatly diminished by the shallower pipe depth. Since the cost of installation of the subsurface soil warming and irrigation system increases greatly with the depth of the pipes, it is recommended that the pipes be placed at a depth of 32.0 cm. It should also be noticed from Figure 26 that the temperature continues to increase for longer periods of operation. It is therefore conceivable that a pipe depth of 32.0 cm would adequately heat the entire root zone for a continuously operated system. As expected, the heating effects increase with decreasing pipe spacing.

Since the heating and irrigation effects increase with decreasing pipe spacing and the cost of the system is proportional to the reciprocal of the pipe spacing, an economic optimization must be performed to find the best pipe spacing. In order to perform such an optimization, one must be able to quantitatively specify the increase in crop yield due to the increased moisture content and temperature produced by the particular spacing. While such an optimization may not be possible, it is felt that an agronomist would find the results of the computer program of great use in selecting a pipe spacing.

While the results of this investigation are thought to be more accurate than other methods available, several improvements are suggested. Comparison of Figures 26 and 27 with the other cases indicates that the temperatures will increase above those calculated for 31 days of operation. It is therefore suggested that any attempt at optimization be based on results calculated for longer periods of operation. It is also felt that further improvements could be obtained by modeling the effects of the plant roots and foliage.

Since the partial differential equations used in this investigation are not thought solvable by exact methods, it is felt that little is to be gained by further efforts to simplify their solution. Experimental work could be similar to that of Reference 13 or could be direct experimental verification of Equations 1 and 2. Such experimental work could resolve the discrepancies reported by Fritton et al.

BIBLIOGRAPHY

1. Boersma, L., and Rykbost, K. A. 1973. Integrated Systems for Utilizing Waste Heat from Steam Electric Plants. Journ. Env. Bull. 2:179-188.

2. Jacob, M. 1949. Heat Transfer. Wiley, Vol. I.

3. Kendricks, J. H., and Havens, J. A. 1971. Heat Budget of a Subsurface Water Pipe Soil Warming System. Water Resources Research Center, University of Arkansas.

4. Philip, J. R., and de Vries, D. A. 1957. Moisture Movement in Porous Materials Under Temperature Gradients. Trans. Am. Geophys. Union 38:222-232.

5. de Vries, D. A. 1958. Simultaneous Transfer of Heat and Moisture in Porous Media. Trans. Am. Geophys. Union 39:909-916.

6. Fritton, D. D., Kirkham, D., and Shaw, R. H. 1970. Soil Water Evaporation, Isothermal Diffusion and Heat and Water Transfer. Soil Sci. Soc. Proc. 34:183-189.

7. Cary, J. W., and Taylor, S. A. 1962. The Interaction of the Simultaneous Diffusions of Heat and Water Vapor. Soil Sci. Soc. Proc. 26:413-416.

8. Cary, J. W., and Taylor, S. A. 1962. Thermally Driven Liquid and Vapor Phase Transfer of Water and Energy in Soil. Soil Sci. Soc. Proc. 26:417-420.

9. Cary, J. W. 1965. Water Flux in Moist Soil: Thermal Versus Suction Gradients. Soil Sci. Soc. Amer. 29:168-175.

10. Rode, A. A. 1969. Theory of Soil Moisture, Vol. I. Israel Program for Scientific Translations, Ltd.

11. Hanks, R. J. 1958. Water Vapor Transfer in Dry Soil. Soil Sci. Soc. Proc. 22:372-374.

12. Sepaskhah, A.R., Boersma, L., Davis, L.R., and Slegel, D.L. 1973. Experimental Analysis of a Subsurface Soil Warming and Irrigation System Utilizing Waste Heat. Paper 73-WA/HT-11, presented at the Winter Annual Meeting ASME, Detroit, Michigan, November 11-15. United Engineering Center, 345 East 47th Street, New York, NY 10017. 12 pp.

13. Sepaskhah, A.R. 1974. Experimental Analysis of Subsurface Heating and Irrigation on the Temperature and Water Content of Soils. Ph.D. Thesis, Oregon State University.

14. Boersma, L. Conversation regarding optimum temperature for plant growth.

15. An Engineering-Economic Study of Cooling Pond Performance. Environmental Protection Agency, May 1970.

16. Kays, W.M. 1966. Convective Heat and Mass Transfer. McGraw-Hill.

17. Laevastu, T. 1960. Factors Affecting the Temperature of the Surface Layer of the Sea. Societas Scientiarum Tennica Comentiones Physico-Mathematicae XXVI. Helsinki.

APPENDICES

APPENDIX I

Empirical Relationships for Solar and Atmospheric Radiation and for the Convective Film Coefficients

The vapor transfer film coefficient was approximated by the Meyer Equation (15, p. 128). It is expressed as

$$q_{evap} = C_{\ell}(0.349)(1.0 + W/10.0)(P_{sat} - P_a) , \qquad (I.1)$$

where W is the wind speed, mph., P_a is the vapor pressure of the atmosphere, C_{ℓ} is a constant, and q_{evap} is the evaporation rate, lb/day-ft^2. The suggested value of C_{ℓ} ranges from 10.0 to 15.0 and was taken to be 10.0. P_{sat} corresponds to the vapor pressure at the surface of the lake and was replaced by the vapor pressure at the soil surface. By assuming that the water vapor behaves as an ideal gas, $P = \rho RT$ and Equation (I.1) may be rewritten as

$$q_{evap} = 3.49(1.0 + W/10.0)(\rho_s R T_s - \rho_a R T_a)$$

or

$$q_{evap} = 3.49\, RT_a(1.0 + W/10.0)(\rho_s T_s/T_a - \rho_a) \qquad (I.2)$$

The surface vapor flux was expressed as

$$q_v = h_D(\rho_s T_s/T_a - \rho_a)$$

and therefore

$$h_D \sim 3.49\, RT_a(1.0 + W/10.0) \qquad (I.3)$$

Since both the vapor and heat are conserved properties (16, p. 315-331), the heat transfer film coefficient is written by analogy between heat and vapor transfer as

$$h = h_D \rho_{air} c_{p_{air}} (\alpha/D)^{2/3}, \qquad (I.4)$$

where α is the thermal diffusivity and D is the diffusivity of the water vapor in air. Although the presence of plants above the soil surface could cause considerable thickening of the boundary layers and, hence, lower film coefficients, it was felt that Equations (I.3) and (I.4) would give acceptable results.

The solar radiation reaching the soil surface has been expressed (17) as

$$q_{rad} = (1.0 - 0.0006\, C^3) q_o, \qquad (I.5)$$

where q_o is the solar radiation reaching the surface on a cloudless day and C is the cloud cover expressed in tenths of the sky covered by clouds.

The atmospheric radiation has been written (15, p. 11) as

$$q_{atm} = \sigma T_a^4 (C_B + 0.223\sqrt{P'_a}), \qquad (I.6)$$

where σ is the Stephan-Boltzman constant and C_B is Brunt's coefficient, which was taken to be 0.66 as an average value (15, p. 12, Figure 3).

APPENDIX II

Closed Form Solution for Test Case

In order to check the results of the computer program, the conduction equation was solved for the following boundary conditions:

$$-\lambda \frac{\partial T}{\partial x} = 0 \quad \text{at} \quad x = 0, \tag{II. 1}$$

$$-\lambda \frac{\partial T}{\partial y} = 0 \quad \text{at} \quad y = 0 \tag{II. 2}$$

$$-\lambda \frac{\partial T}{\partial y} = h(T-T_\infty) \quad \text{at} \quad y = 48 \text{ cm} \tag{II. 3}$$

$$-\lambda \frac{\partial T}{\partial x} = q(y) \quad \text{at} \quad x = 40 \text{ cm} \tag{II. 4}$$

$$T = T_o \quad \text{at} \quad x = 40 \text{ cm} \quad \text{and} \quad y = 12 \text{ cm} \tag{II. 5}$$

The conduction equation for constant thermal conductivity is $\nabla^2 T = 0$, which for $T - T_\infty = F(x)\ G(y)$ becomes

$$F''G + FG'' = 0 \tag{II. 6}$$

The solutions for $F(x)$ and $G(y)$ are

$$F(x) = A_i \cosh(\gamma_i x) + B_i \sinh(\gamma_i x) \tag{II. 7}$$

$$G(y) = C_i \cos(\gamma_i y) + D_i \sin(\gamma_i y) \tag{II. 8}$$

Application of B.C. 1 yields $B_i = 0$, and B.C. 2 yields $D_i = 0$. Use

of B.C.3 leads to

$$\mathrm{Tan}(\beta_i) = \alpha/\beta_i \,, \tag{II.9}$$

where

$$\alpha = 48h/\lambda \,,$$

and

$$\beta_i = 48\gamma_i \,.$$

In order to apply B.C.4, $q(y)$ is chosen to represent an insulated side with an unspecified heat flux at one node. The term, $q(y)$ is then

$$\begin{aligned} q &= 0 \quad \text{when} \quad y < 10 \text{ cm}, \quad y > 14 \text{ cm} \\ q &= q_o \quad \text{when} \quad 10 < y < 14 \text{ cm}. \end{aligned} \tag{II.10}$$

Use of B.C.4, and Equation (II.10) leads to the following expression for $E_i = A_i C_i$,

$$E_i = \frac{196 q_o [\sin(7\beta_i/24) - \sin(5\beta_i/24)]}{\lambda \beta_i \sinh(5\beta_i/6)[2\beta_i + \sin(2\beta_i)]} \tag{II.11}$$

Use of B.C.5 yields

$$T_o = \sum_{i=1}^{\infty} E_i \cos(\beta_i/4) \cosh(5\beta_i/6) \tag{II.12}$$

Elimination of q_o from Equations (II.11) and (II.12) yields

$$T(x, y) = \frac{T_o}{P} \sum_{i=1}^{\infty} \frac{\cos(\beta_i\, y/48)\ [\sin(7\beta_i/24) - \sin(5\beta_i/24)]}{\beta_i \sinh(5\beta_i/6)[\,2\beta_i + \sin(2\beta_i)]} \cosh(\beta_i \frac{x}{48}) \tag{II. 13}$$

where

$$P = \sum_{i=1}^{\infty} \frac{\cos(\beta_i/4)[\sin(7\beta_i/24) - \sin(5\beta_i/24)]}{\beta_i \tanh(5\beta_i/6)[2\beta_i + \sin(2\beta_i)]} \tag{II. 14}$$

APPENDIX III

Computer Program Listing and Data Input Explanation

```
      PROGRAM GREEN
      DIMENSION T(45,20),THETA(45,20),TC(45,20),THO(45,20),
     1EVAP(45,20)
      COMMON DELTAZ,DELTAT,DELZ2,TEMP
      DATA (EVAP=900(0.0)),(THETA=900(0.45))
      S=0.45
      DELTAZ=10.0
      READ(60,990) DELTAT,TMAX
C  FTS,FTH,FF,FS1 ARE NORMALLY 1.0, FOR STEADY-STATE CASES
C    SET HIGHER TO ACCELERATE CONVERGENCE
C  FTH+FTS ARE THETA FUDGE FACTORS
      READ(60,990) FTS
      READ(60,990) FTH
      READ(60,990)FF
      READ(60,990)FS1
      READ(60,990) R2,RZ2C
C R2= DELTAZ/DELTAY SQUARED AND SHOULD BE SET LESS THAN
C    1.0 FOR CONVERGENCE
C RZ2C =THE SQUARE OF DELTAZ/DELTAZ IN THE SATURATED REGION
      WRITE(61,990) DELTAT,DELTAZ,R2
      READ(60,990) TEMP
C TEMP= AN ARBITRARY DIFFERENCE IN TEMPERATURE AND WAS USED
C    TO NON-DIMENSIONALIZE
      READ(60,991) MPIPE1,MPIPE,MMAX,NMAX,MBOUND
C MPIPE= THE LEFT PIPE LOCATION
C MPIPE1 IS THE RIGHT PIPE LOCATION
C MMAX IS THE NUMBER OF GRID LEVELS IN THE Z DIRECTION
C NMAX IS THE NUMBER OF GRID LEVELS IN THE Y DIRECTION
C MBOUND IS THE LEVEL BELOW WHICH THE GROUND IS SATURATED
C  NO THETA CALCULATIONS ARE MADE BELOW MBOUND
      READ(60,991) ISTART
C  ISTART IS ZERO WHEN THE STEP IS APPLIED AT THE PIPE
C   IE, WHEN THE IRRIGATION STARTS
      BCSOIL=0.335
      DELZ2=DELTAZ*DELTAZ
      CALL PSII(PSI,TE,TH1)
      CALL BETAA(BETA,TE)
      CALL LAMDA(DLAM,TE)
      HFG=2450.0/4.1868/TEMP
      R=8.3143/1.8/0.98*TEMP/DELTAZ*11.0**3
      TIME=0.0
      DO 2 M=1,MMAX
 2    READ(21,990) (T(M,N),N=1,NMAX)
C  THESE TEMPERATURES ARE NON-DIMENSIONALIZED AND =T/TEMP
      DO 1 M=MBOUND,MMAX
 1    READ(21,990) (THETA(M,N),N=1,NMAX)
C  EPS IS THE SOIL EMMISIVITY
      EPS=0.4
      IF(ISTART.EQ.0) THETA(MPIPE1,NMAX)=0.44
      IF(ISTART.EQ.0) T(MPIPE1,NMAX)=46.398
      IF(ISTART.EQ.0) T(MPIPE,1)=47.923
      IF(ISTART.EQ.0) THETA(MPIPE,1)=0.44
```

```
C THESE ARE THE PIPE CONDITIONS
      SIG=TEMP**3*DELTAT/DELTAZ*5.67/4.186/10.0**12
      MMM=MMAX-1
 10   CALL WEATHR(TIME,H,HO,T8,B8,GRAD,RAIN)
C WEATHR CALCULATES THE ATMOSPHERIC CONDITIONS
C IT ALSO CALCULATES FILM COEFFICIENTS
      DO 430 M=2,MMAX
      DO 430 N=1,NMAX
 430  TO(M,N)=T(M,N)
      DO 431 M=1,MMAX
      DO 431 N=1,NMAX
 431  THO(M,N)=THETA(M,N)
C TO AND THO ARE THE TEMPERATURES AND WATER CONTENTS
C    AT THE LAST TIME STEP
 201  DO 100 M=MBCONC,MMM
      DO 100 N=1,NMAX
C  THIS LOOP CALCULATES THE DEL.C*DEL(RHO)
C  WHICH IS THE EVAPORATION RATE WITHOUT THE TRANSIENT TERM
      T1=T(M,N)
      TH1=THETA(M,N)
      T2=T(M+1,N)
      TH2=THETA(M+1,N)
      T3=T(M-1,N)
      TH3=THETA(M-1,N)
      T4=T(M,N+1)
      TH4=THETA(M,N+1)
      IF(N.EQ.1) GO TO 35
      T5=T(M,N-1)
      TH5=THETA(M,N-1)
      IF(N.NE.NMAX) GO TO 40
      IF(M.EQ.MPIPE1) GO TO 100
      T4=T5
      TH4=TH5
      GO TO 40
 35   IF(M.EQ.MPIPE) GO TO 100
      T5=T4
      TH5=TH4
 40   CONTINUE
      TE=T1
      CALL PSII(PSI,TE,TH1)
      CALL BETAA(BETA,TE)
      B1=BETA*EXP(PSI/TE/R)
      TE=T2
      CALL BETAA(BETA,TE)
      CALL PSII(PSI,TE,TH2)
      B2=BETA*EXP(PSI/TE/R)
      TE=T3
      CALL BETAA(BETA,TE)
      CALL PSII(PSI,TE,TH3)
      B3=BETA*EXP(PSI/TE/R)
      TE=T4
      CALL BETAA(BETA,TE)
```

```
      CALL PSII(PSI,TE,TH4)
      B4=BETA*EXP(PSI/TE/R)
      TE=T5
      CALL BETAA(BETA,TE)
      CALL PSII(PSI,TE,TH5)
      B5=BETA*EXP(PSI/TE/R)
      TT=(TH2+TH1)/2.0
      TE=(T2+T1)/2.0
      DD=DIFFUS(TE,TT)*(B2-B1)
      TT=(TH3+TH1)/2.0
      TE=(T3+T1)/2.0
      DD=DD+DIFFUS(TE,TT)*(B3-B1)
      TE=(T4+T1)/2.0
      TT=(TH4+TH1)/2.0
      DD=DD+DIFFUS(TE,TT)*(B4-B1)*R2
      TE=(T5+T1)/2.0
      TT=(TH5+TH1)/2.0
      DD=DD+DIFFUS(TE,TT)*(B5-B1)
  100 EVAP(M,N)=-DD
      M=MMAX
C EVAPORATION AT THE SURFACE
      DO 110 N=1,NMAX
      T1=T(M,N)
      TH1=THETA(M,N)
      T3=T(M-1,N)
      TH3=THETA(M-1,N)
      T4=T(M,N+1)
      TH4=THETA(M,N+1)
      IF(N.EQ.1) GO TO 135
      T5=T(M,N-1)
      TH5=THETA(M,N-1)
      IF(N.NE.NMAX) GO TO 140
      T4=T5
      TH4=TH5
      GO TO 140
  135 T5=T4
      TH5=TH4
  140 CONTINUE
      TE=T1
      CALL PSII(PSI,TE,TH1)
      CALL BETAA(BETA,TE)
      B1=BETA*EXP(PSI/TE/R)
      TE=T3
      CALL BETAA(BETA,TE)
      CALL PSII(PSI,TE,TH3)
      B3=BETA*EXP(PSI/TE/R)
      TE=T4
      CALL BETAA(BETA,TE)
      CALL PSII(PSI,TE,TH4)
      B4=BETA*EXP(PSI/TE/R)
       TE=T5
      CALL BETAA(BETA,TE)
```

```
      CALL PSII(PSI,TE,TH5)
      B5=BETA*EXP(PSI/TL/R)
      TT=(TH3+TH1)/2.0
      TE=(T3+T1)/2.0
      DD=DIFFUS(TE,TT)*(B3-B1)*2.0
      TE=(T4+T1)/2.0
      TT=(TH4+TH1)/2.0
      CD=DIFFUS(TE,TT)*(B4-B1)*RZ
      TE=(T5+T1)/2.0
      TT=(TH5+TH1)/2.0
      CD=DD+DIFFUS(TE,TT)*(B5-B1)+2.0*HD*(B8-B1*T1/T8)
  110 EVAP(M,N)=-DD
      DIF=0.0
      KKK=0
      RZ2=RZ20
C  THIS LOOP CALCULATES THE TEMPERATURES
      DO 210 M=2,MMM
      DO 210 N=1,NMAX
      IF(M.GE.MBOUND) RZ2=1.0
      TH1=THO(M,N)
      TE=TO(M,N)
      CALL PSII(PSI,TE,TH1)
      CALL BETAA(BETA,TE)
      B1=BETA*EXP(PSI/TE/R)
      TE=TE+1.0
      CALL BETAA(BETA,TE)
      CALL PSII(PSI,TE,TH1)
      BS=BETA*EXP(PSI/TE/R)
      BS=BS-B1
      T1=T(M,N)
      TH1=THETA(M,N)
      T2=T(M+1,N)
      TH2=THETA(M+1,N)
      T3=T(M-1,N)
C     IF(M.EQ.2) T3=T2
C    USE FOR INSULATED BOUNDARY
      TH3=THETA(M-1,N)
      T4=T(M,N+1)
      TH4=THETA(M,N+1)
      IF(N.EQ.1) GO TO 235
      T5=T(M,N-1)
      TH5=THETA(M,N-1)
      IF(N.NE.NMAX) GO TO 240
      IF(M.EQ.MPIPE1) GO TO 210
      T4=T5
      TH4=TH5
      GO TO 240
  235 IF(M.EQ.MPIPE) GO TO 210
      T5=T4
      TH5=TH4
  240 CONTINUE
      TE=(TH2+TH1)/2.0
```

```
      CALL LAMDA(DLAM,TE)
      CIV=DLAM*RZ2
      D=DLAM*T2*RZ2
      TE=(TH3+TH1)/2.0
      CALL LAMDA(DLAM,TE)
      C=D+DLAM*T3*RZ2
      DIV=DIV+DLAM*RZ2
      TE=(TH4+TH1)/2.0
      CALL LAMDA(DLAM,TE)
      DIV=DIV+DLAM*R2
      D=D+DLAM*T4*R2
      TE=(TH5+TH1)/2.0
      CALL LAMDA(DLAM,TE)
      C=D+DLAM*T5*R2
      DIV=DIV+DLAM*R2
      TE=T2
      CALL PSII(PSI,TE,TH2)
      TT=T3
      CALL PSII(PST,TT,TH3)
      DD=(TE-TT)*(PSI-PST+2.0)*RZ2
      TE=T4
      TT=T5
      CALL PSII(PSI,TE,TH4)
      CALL PSII(PST,TT,TH5)
      DD=DD+(TE-TT)*(PSI-PST)*R2
      D=D+DD*CAY(TH1)/4.0
      T(M,N)=D+TO(M,N)*(TH1+BCSOIL+(S-TH1)*BS*HFG)
     1 -EVAP(M,N)*HFG
      DIV=DIV+TH1+BCSOIL+BS*(S-TH1)*HFG
      T(M,N)=T(M,N)/DIV
      T(M,N)=T(M,N)*FS1+T1*(1.0-FS1)
      DIV=T1
      T1=T(M,N)
      CALL BETAA(BETA,T1)
      CALL PSII(PSI,T1,TH1)
      BS=BETA*EXP(PSI/T1/R)
      EVAP(M,N)=EVAP(M,N)+(S-TH1)*(BS-B1)
  210 DIF=DIF+ABS(T(M,N)/DIV-1.0)
      M=MMAX
C  THIS LOOP CALCULATES THE TEMPERATURES AT THE SURFACE
      DO 220 N=1,NMAX
      T1=T(M,N)
      TE=TO(M,N)
      TH1=THO(M,N)
      CALL PSII(PSI,TE,TH1)
      CALL BETAA(BETA,TE)
      B1=BETA*EXP(PSI/TE/R)
      TE=TE+1.0
      CALL BETAA(BETA,TE)
      CALL PSII(PSI,TE,TH1)
      BS=BETA*EXP(PSI/TE/R)
      BS=BS-B1
```

```
      TH1=THETA(M,N)
      T3=T(M-1,N)
      TH3=THETA(M-1,N)
      T4=T(M,N+1)
      TH4=THETA(M,N+1)
      IF(N.EQ.1) GO TO 255
      T5=T(M,N-1)
      TH5=THETA(M,N-1)
      IF(N.NE.NMAX) GO TO 260
      T4=T5
      TH4=TH5
      GO TO 260
  255 T5=T4
      TH5=TH4
  260 D=2.0*EPS*QRAD-EPS*SIG*T1**4
      TE=(TH3+TH1)/2.0
      CALL LAMDA(DLAM,TE)
      D=D+DLAM*2.0*T3+2.0*H*T8
      DIV=2.0*DLAM+2.0*H+EPS*SIG*T1**3
      TE=(TH4+TH1)/2.0
      CALL LAMDA(DLAM,TE)
      D=D+DLAM*T4*R2
      DIV=DIV+DLAM*R2
      TE=(TH5+TH1)/2.0
      CALL LAMDA(DLAM,TE)
      DIV=DIV+DLAM*R2
      D=D+DLAM*T5*R2
      TT=(TH1+TH3)/2.0
      CO=CAY(TT)
      CALL PSII(PSI,T1,TH1)
      CALL PSII(PST,T3,TH3)
      D=D+2.0*CO*T3*(PSI-PST+1.0)+2.0*RAIN*T8
      DIV=DIV+2.0*CO*(PSI-PST+1.0)+2.0*RAIN
      TE=T4
      TT=T5
      CALL PSII(PSI,TE,TH4)
      CALL PSII(PST,TT,TH5)
      C=D+(TE-TT)*(PSI-PST)*R2*CAY(TH1)/4.0
      T(M,N)=D+TO(M,N)*(TH1+BCSOIL+(S-TH1)*BS*HFG)
     1 -EVAP(M,N)*HFG
      DIV=DIV+TH1+BCSOIL+BS*(S-TH1)*HFG
      T(M,N)=T(M,N)/DIV
      T(M,N)=T(M,N)*FF+T1*(1.0-FF)
      DIV=T1
      T1=T(M,N)
      CALL BETAA(BETA,T1)
      CALL PSII(PSI,T1,TH1)
      BS=BETA*EXP(PSI/T1/R)
      EVAP(M,N)=EVAP(M,N)+(S-TH1)*(BS-B1)
  220 DIF=DIF+ABS(T(M,N)/DIV-1.0)
  202 DIF1=0.0
C THIS LOOP CALCULATES WATER CONTENTS
```

```
      DO 300 M=MBOUND,MMM
      DO 300 N=1,NMAX
      T1=T(M,N)
      TT=THETA(M,N)
      NUM=0
      FSI=0.0006
C FSI IS A FUDGE FACTOR AND VARIES WITH THETA
C  ITS VALUE MUST BE FOUND BY TRIAL AND ERROR FOR A
C  PARTICULAR COMBINATION OF DELTAT,DELTAZ ETC
C   THESE PARTICULAR VALUES ARE FOR DELTAT= 1.0 DAY
C     AND DELTAZ=10.0 CM
      IF(TT.LT.0.44) FSI=0.0006
      IF(TT.LT.0.42) FSI=0.001
      IF(TT.LT.0.41) FSI=0.00125
      IF(TT.LT.0.40) FSI=0.0021
      IF(TT.LT.0.39) FSI=0.00225
      IF(TT.LT.0.385)FSI=0.0055
      IF(TT.LT.0.35) FSI=0.007
      IF(TT.LT.0.32) FSI=0.009
      IF(TT.LT.0.30) FSI=0.013
      IF(TT.LT.0.29) FSI=0.03
      IF(TT.LT.0.25) FSI=0.06
      IF(TT.LT.0.20) FSI=0.08
C   SINCE THETA VARIES GREATLY NEAR THE PIPE WHEN
C     THE IRRIGATION STARTS, A SMALL FUDGE FACTOR
C     IS USED
      IF(ISTART.GT.0) GO TO 998
      KK=MPIPE-1
      IF(M.EQ.KK) FSI=0.0008
      KK=MPIPE+1
      IF(M.EQ.KK) FSI=0.0008
      IF(M.EQ.MPIPE) FSI=0.0008
 998  DDD=TT
      T2=T(M+1,N)
      TH2=THETA(M+1,N)
      T3=T(M-1,N)
      TH3=THETA(M-1,N)
      T4=T(M,N+1)
      TH4=THETA(M,N+1)
      IF(N.EQ.1) GO TO 305
      T5=T(M,N-1)
      TH5=THETA(M,N-1)
      IF(N.NE.NMAX) GO TO 309
      IF(M.EQ.MPIPE1) GO TO 300
      T4=T5
      TH4=TH5
      GO TO 309
 305  IF(M.EQ.MPIPE) GO TO 300
      T5=T4
      TH5=TH4
 309  CONTINUE
      TH1=THO(M,N)-EVAP(M,N)
```

```
 305  CONTINUE
      DIV=TT
      TE=(TT+TH2)/2.0
      CALL PSII(PST,T2,TH2)
      CALL PSII(PSI,T1,TT)
      DD=CAY(TE)*(PST-PSI+1.0)
      TE=(TH4+TT)/2.0
      CALL PSII(PST,T4,TH4)
      DD=DD+CAY(TE)*(PST-PSI)*R2
      TE=(TT+TH3)/2.0
      CALL PSII(PST,T3,TH3)
      DD=DD+CAY(TE)*(PST-PSI-1.0)
      TE=(TH5+TT)/2.0
      CALL PSII(PST,T5,TH5)
      DD=DD+CAY(TE)*(PST-PSI)*R2
      TT=(1.0-PSI)*TT+(TH1+DD)*PSI
      DIV=ABS((TH1+DD)/DIV-1.0)
      NUM=NUM+1
      IF(NUM.GT.20) GO TO 300
C     TWENTY-ONE ITERATIONS MAXIMUM
      IF(DIV.GT.0.00001) GO TO 305
C THIS IS THE CONVERGENCE CRITERIA FOR EACH VALUE OF THETA
      DIF1=DIF1+ABS(TT/DDD-1.0)
 300  THETA(M,N)=(1.0-FTH)*THETA(M,N)+TT*FTH
      M=MMAX
C THIS LOOP CALCULATES WATER CONTENTS AT THE SURFACE
      DO 310 N=1,NMAX
      T1=T(M,N)
      TH1=THETA(M,N)
      NUM=0
      FS=0.01
C FS  IS SIMILAR TO FSI
      IF(TH1.LT.0.255) FS=0.09
      IF(TH1.LT.0.215) FS=0.035
      IF(TH1.LT.0.190) FS=0.08
      IF(TH1.LT.0.150) FS=0.1
      IF(TH1.LT.0.13) FS=0.05
      DDD=TH1
      T3=T(M-1,N)
      TH3=THETA(M-1,N)
      T4=T(M,N+1)
      TH4=THETA(M,N+1)
      IF(N.EQ.1) GO TO 335
      T5=T(M,N-1)
      TH5=THETA(M,N-1)
      IF(N.NE.NMAX) GO TO 340
      T4=T5
      TH4=TH5
      GO TO 340
 335  T5=T4
      TH5=TH4
 340  CONTINUE
```

```
      CALL PSII(PSI,T1,TH1)
      TE=(TH4+TH1)/2.0
      CALL PSII(PST,T4,TH4)
      DD=-EVAP(M,N)+2.0*RAIN+CAY(TE)*(PST-PSI)*R2+THC(M,N)
      TE=(TH1+TH3)/2.0
      CALL PSII(PST,T3,TH3)
      DD=DD+2.0*CAY(TE)*(PST-PSI-1.0)
      TE=(TH5+TH1)/2.0
      CALL PSII(PST,T5,TH5)
      DD=DD+CAY(TE)*(PST-PSI)*R2
      TH1=(1.0-FS)*TH1+DD*FS
      DD=ABS(DD/TH1-1.0)
      NUM=NUM+1
      IF(NUM.EQ.20) GO TO 310
      IF(DD.GT.0.00001) GO TO 341
C THIS IS THE CONVERGENCE CRITERIA FOR EACH VALUE OF THETA
      DIF1=DIF1+ABS(TH1/DDD-1.0)
  310 THETA(M,N)=(1.0-FTS)*DDD+FTS*TH1
      DIF1=DIF1/NMAX/(MMAX-MBOUND)
      DIF=DIF/MMAX/NMAX
      KKK=KKK+1
      WRITE(61,990) DIF,DIF1
C     THE THETA ARRAY CONVERGES MORE SLOWLY THAN THE
C     TEMPERATURE ARRAY.  IF THE TEMPERATURES HAVE
C     CONVERGED, KKK ALLOWS FOUR EXTRA ITERATIONS FOR
C     THETA BEFORE ITERATING AGAIN ON TEMPERATURE
      IF(KKK.EQ.5) GO TO 201
      IF(DIF.GT.0.00012) GO TO 201
      IF(DIF1.GT.0.0006) GO TO 202
C     DIF + DIF1 ARE PERCENT CHANGE IN THE ARRAYS
C   THEY ARE CALCULATED AS FRACTIONS OF THE ABSOLUTE
C        VALUE OF THE VARIABLE
C SINCE TEMPERATURE IS ABSOLUTE(KELVIN)  DIF SHOULD
C     BE SMALLER THAN DIF1
      TIME=TIME+1
      IF(TIME.LT.TMAX) GO TO 10
      DO 415 M=1,MMAX
  415 WRITE(21,990) (T(M,N),N=1,NMAX)
      DO 420 M=MBOUND,MMAX
  420 WRITE(21,990) (THETA(M,N),N=1,NMAX)
  990 FORMAT(3X,8E13.7)
  991 FORMAT(5I2)
      END

      SUBROUTINE PSII(C,T,TE)
      DIMENSION TKT(20),CKT(20), TK(21),CK(20)
      COMMON DELTAZ,DELTAT,DELZ2,TEMP
      DATA (KI=0)
      IF(KI.EQ.1) GO TO 11
      KI=1
      I=1
    3 READ(60,111) TKT(I),CKT(I),LAST
```

```
      CKT(I)=CKT(I)/.980665*1000.0/DELTAZ
      I=I+1
      IF(LAST.EQ.0) GO TO 3
      ITMAX=I-1
      I=1
 4    READ(60,111) TK(I),CK(I),LAST
      TK(I)=TK(I)+273.16
      TK(I)=TK(I)/TEMP
      CK(I)=CK(I)/72.75
C     72.75 IS THE SURFACE TENSION AT 20 DEGREES
      I=I+1
      IF(LAST.EQ.0) GO TO 4
      JMAX=I-1
      I=1
      J=1
      RETURN
 111  FORMAT(2F10.0,I2)
  11  IF(TE.LT.TKT(I)) GO TO 15
      I=I+1
      IF(I.GT.ITMAX) GO TO 300
      GO TO 11
  15  IF(TE.GT.TKT(I)) GO TO 20
      I=I-1
      IF(I.EQ.0) GO TO 300
      GO TO 15
  20  C=CKT(I)+(CKT(I+1)-CKT(I))*(TE-TKT(I))/(TKT(I+1)
     1 -TKT(I))
 8    IF(T.LT.TK(J)) GO TO 9
      J=J+1
      IF(J.GT.JMAX) GO TO 300
      GO TO 8
 9    IF(T.GT.TK(J)) GO TO 30
      J=J-1
      IF(J.EQ.0) GO TO 300
      GO TO 9
 30   CC=CK(J)+(CK(J+1)-CK(J))*(T-TK(J))/(TK(J+1)-TK(J))
      C=C*CC
      RETURN
 300  WRITE(61,301)
 301  FORMAT(# SEARCH HAS EXCEEDED FILE-PS1#)
      GO TO 3
      END

      FUNCTION DIFFUS(TT,THET)
      COMMON DELTAZ,DELTAT,DELZ2
      S=0.49
      D=0.239*(TT/281.16)**2.3
      D=D*(S-THET)
      DIFFUS=D*DELTAT/DELZ2
      RETURN
      END
```

```
      FUNCTION CAY(TH)
      COMMON DELTAZ,DELTAT,DELZ2
      B=2.9
      C=0.069/60.0*DELTAT/DELTAZ
      TS=0.49
      B=B*2.0+2.0
      CAY=C*(TH/TS)**B
      IF(TH.GE.TS) CAY=C
      RETURN
      END

      SUBROUTINE LAMCA(C,TE)
      DIMENSION TKT(50),CKT(50)
      COMMON DELTAZ,DELTAT,DELZ2
      DATA (KI=0)
      IF(KI.EQ.1) GO TO 11
      I=1
      KI=1
  3   READ(60,111) TKT(I),CKT(I),LAST
      CKT(I)=CKT(I)*DELTAT/DELZ2/1000.0
      TKT(I)=TKT(I)*1.69
      I=I+1
      IF(LAST.EQ.0) GO TO 3
      ITMAX=I-1
      I=1
      RETURN
111   FORMAT(2F10.0,I2)
 11   IF(TE.LT.TKT(I)) GO TO 15
      I=I+1
      IF(I.GT.ITMAX) GO TO 300
      GO TO 11
 15   IF(TE.GT.TKT(I)) GO TO 20
      I=I-1
      IF(I.EQ.0) GO TO 300
      GO TO 15
 20   C=CKT(I)+(CKT(I+1)-CKT(I))*(TE-TKT(I))/(TKT(I+1)
     1 -TKT(I))
      RETURN
 300  WRITE(61,301)
 301  FORMAT(* SEARCH HAS EXCEEDED FILE-LAMDA*)
      GO TO 3
      END

      SUBROUTINE BETAA(C,TE)
      DIMENSION TKT(50),CKT(50)
      COMMON DELTAZ,DELTAT,DELZ2,TEMP
      DATA (KI=0)
      IF(KI.EQ.1) GO TO 10
      KI=1
      I=1
  3   READ(60,111) TKT(I),CKT(I),LAST
      CKT(I)=1.0/CKT(I)
```

```
      TKT(I)=TKT(I)+273.16
      TKT(I)=TKT(I)/TEMP
      I=I+1
      IF(LAST.EQ.0) GO TO 3
      ITMAX=I-1
      I=1
      RETURN
  111 FORMAT(2F10.0,I2)
  10  IF(TE.LT.TKT(I)) GO TO 15
      I=I+1
      IF(I.GT.ITMAX) GO TO 300
      GO TO 10
  15  IF(TE.GT.TKT(I)) GO TO 20
      I=I-1
      IF(I.EQ.0) GO TO 300
      GO TO 15
  20  C=CKT(I)+(CKT(I+1)-CKT(I))*(TE-TKT(I))/(TKT(I+1)
     1 -TKT(I))
      RETURN
  300 WRITE(61,301)
  301 FORMAT(* SEARCH HAS EXCEEDED FILE-BETA*)
      GO TO 3
      END

      SUBROUTINE WEATHR(TIME,H,HC,TA,BB,GRAD,RAIN)
      COMMON DELTAZ,DELTAT,DELZ2,TEMP
      DATA (KI=0)
      IF(KI.EQ.1) GO TO 2
      SIG=TEMP**3*DELTAT/DELTAZ*5.67/4.186/10.0**12
      RR=82.05/18.0*14.7*TEMP
      CPAIR=0.24
C****** R=PRESSURE*TEMP/GAS CONSTANT
      R=28.96/82.054/TEMP
      C2=0.185*0.508**2*TEMP/68.0*9.0/5.0*DELTAT/DELZ2
      C1=0.72*(0.508)**2*DELTAT/DELZ2
      T0=273.16/TEMP
      THETAA=0.0
      S=0.49
      KI=1
      G=980.
  101 FORMAT(5F5.2)
  2   READ(20,101) TA,DE,CLOUD,RAIN,EE
      CLOUD=(CLOUD/10.0)**3
      GRAD=2.0*(1.0-0.6*CLOUD)*DELTAT/DELTAZ/TEMP/60.0/3.14
      RAIN=RAIN*2.54/DELTAZ/24.0/3600.0*DELTAT
      TA=TA-32.0
      TA=TA*5.0/9.0+273.16
      TA=TA/TEMP
      RHOAIR=R/TA
      ALPHA=C1+C2*(TA-T0)
      CALL BETAA(BB,TA)
      BB=BB*BB/100.0
```

```
PA=RR*BB*TA
QRAD=QRAD+SIG*TA**4*(0.66+0.223*SQRT(PA))
D=DIFFUS(TA,THETAA)
D=D/S
HD=3.49*(1.0+UB/10.0)*RR*TA
HD=HD/7200.0*2.54/62.4
HD=HD*DELTAT/DELTAZ
H=HD*RHOAIR*CPAIR*(ALPHA/D)**0.666
RETURN
END
```

Typical Input Data

File 60

Records one through seven have a format of 3x, 2E13.7, records eight and nine have format 5I2, and the remaining records have a format of 2F10.0, I2. Record one contains the time step in seconds and the number of time steps to be calculated for a particular execution of the computer program. Records two through five are factors for accelerating convergence for steady-state solutions. Record six contains the factors (deltaz/deltay) squared, and (deltaz/deltaz in the saturated region) squared. Record seven contains the arbitrary temperature increment used to non-dimensionalize the governing equations. Record eight contains, in order, the right-hand pipe depth, the left-hand pipe depth, the number of nodes in the vertical direction, the number of nodes in the horizontal direction, and the index of the node below which the soil is assumed saturated. Record nine contains an indicator as to whether the pipe operation is starting. The indicator is blank or zero if operation is starting and any positive number if operation is not starting.

Following record nine are data groups for the soil properties and for the specific volume of water vapor. The last record of each data group contains a positive number in columns 11 or 12. The first data group is for potential. Moisture content (cm^3/cm^3) is the first

variable and potential (bars) is the second variable. The data is assumed to be obtained at a temperature of 20 C. The second data file contains temperature (°C) and then surface tension (Dynes/cm). The third data group contains temperature (°C) and specific volume (cm^3/g). The fourth and last data group contains moisture content (grams of moisture/gram of dry soil) and thermal conductivity (millicalories/cm-sec-C).

A sample data deck is presented below.

```
    86400.0          31.0
    1.0
    1.0
    1.0
    1.0
    1.0                0.04
    1.0
0135451525
0.0645       -15.0
          .
          .
          .
0.461        -0.04977    99
0.0          75.6
          .
          .
          .
50.0         67.91       99
2.0          179889.0
          .
          .
          .
50.0         12032.0     99
0.0          0.6
          .
          .
          .
0.236        4.15        99
```

File 20

The format is 5F5.2 and there is one record for each time step. For the card shown below, the ambient temperature is 38.93 F, the average wind speed is 9.90 mph, the cloud cover is 8.39 tenths, the precipitation is .2 inches/day, and the relative humidity is 81.90 percent.

```
38.93 9.90 8.39 .2081.90
  :
  :
  :
```

File 21

The format is 3x, 8E13.7 and the data in this file is the initial temperature and moisture content arrays. Each horizontal row of nodes is listed consecutively beginning with the deepest row. The temperature array is listed first and then the moisture content array. After execution of the program, the final temperature and moisture content arrays are written on the file after the initial arrays. For the typical data shown in File 60, the temperature array would contain 90 lines of data. Two lines of data are needed for each node level because the array size is 15 horizontally and the format allows 8 values per line. The moisture content array would contain 42 lines of data because initial data for 21 node levels is needed.